

Damage and strength predictions of 3D woven composite structures: state-of-the-art and perspectives

F. Laurin, A. Hurmane, V. Medeau, J. Rannou



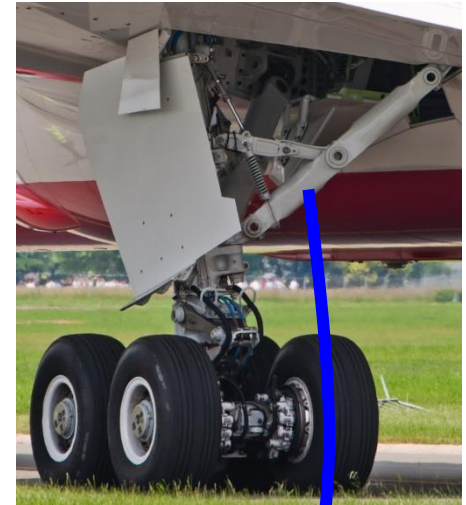
r e t u r n o n i n n o v a t i o n

Industrial context : 3D woven composites

LEAP engine



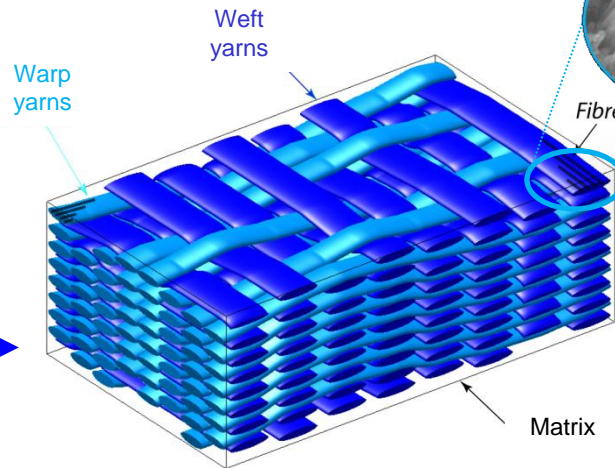
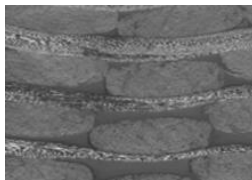
Landing gear



Safran Aircraft Engines Safran Landing Systems

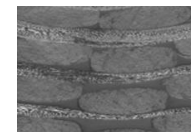
- 3D woven with polymer matrix
 - Structures subjected to impact
 - Fan blade, Carter, Lug
- Need of comprehension
 - Recent materials, recently certified
- Physically based model needed

Fan blade
3D woven
PMC

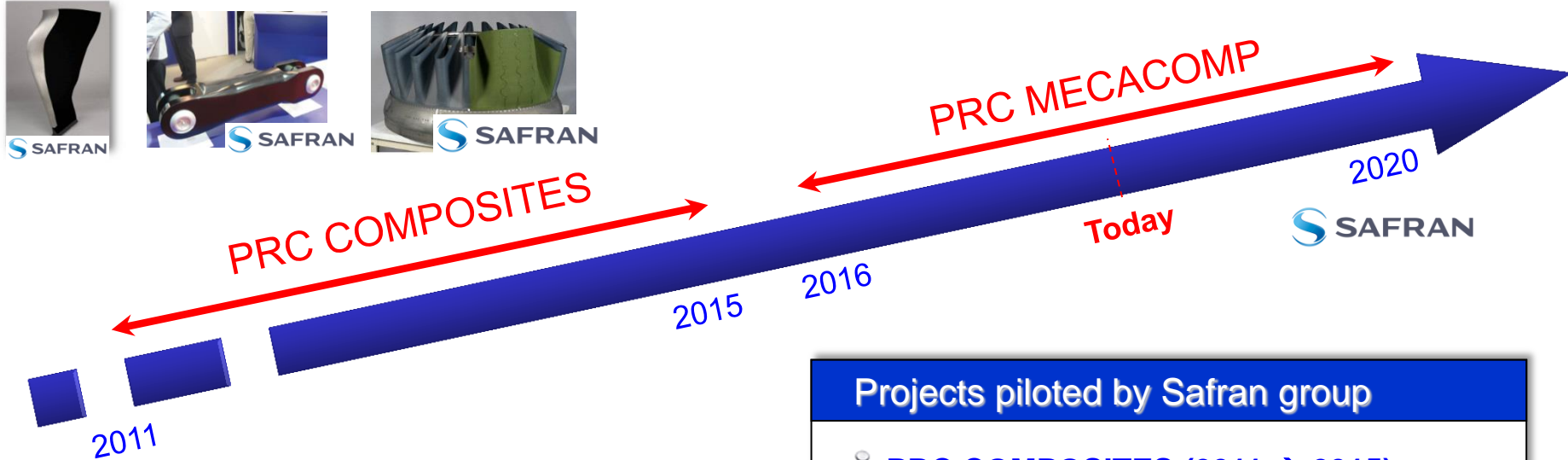


3D woven composite materials

Lug
3D woven
PMC

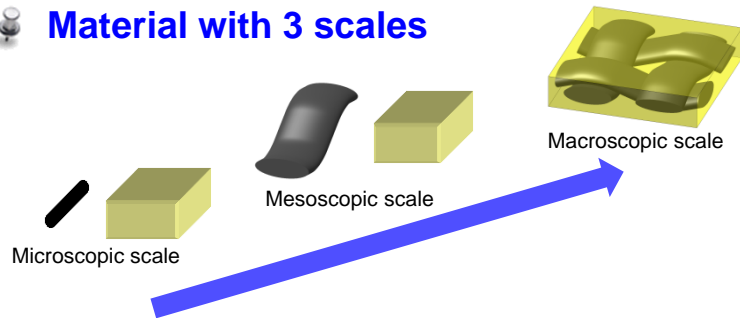


Industrial context : National research projects



Multiscale composite materials

Material with 3 scales



Macroscopic scale for design composite structures in aeronautical industries

Projects piloted by Safran group

PRC COMPOSITES (2011 → 2015)

French Research project financed by DGAC involving Safran Group, Onera and CNRS

~20 Phd-theses in different laboratories:
[\[Rakotoarisoa 13\]](#), [\[Hemon 13\]](#), [\[Hurmane 15\]](#),
[\[Elias 15\]](#), [\[Mounien 17\]](#) ...

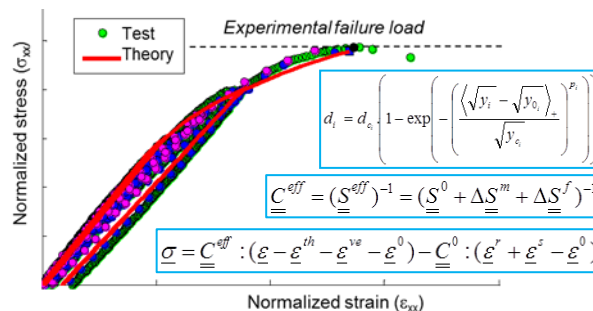
PRC MECACOMP (2016 → 2020)

French Research project financed by DGAC involving Safran Group, Onera and CNRS

~20 Phd-theses in different laboratories:
[\[Medeau19\]](#), [\[Garcia 19\]](#), [\[Sally 20\]](#),
[\[Archer 20\]](#) ...

Three main steps for a robust design approach

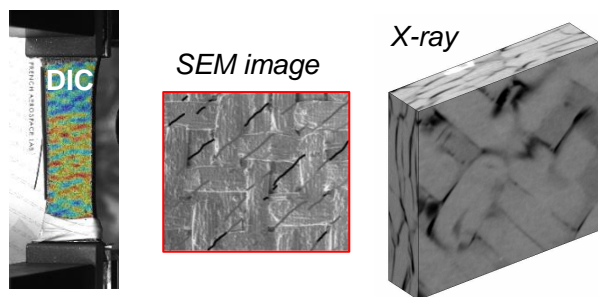
Material modelling



Proposition of material models

- Damage modelling
- Fibre failure, softening behaviour

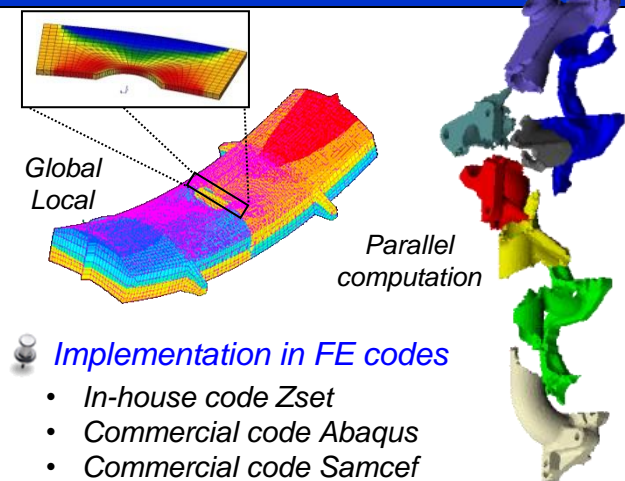
Characterization tests



Comprehension of ϕ mechanisms

- Acoustic emission
- Digital image correlation
- X-Ray Tomography

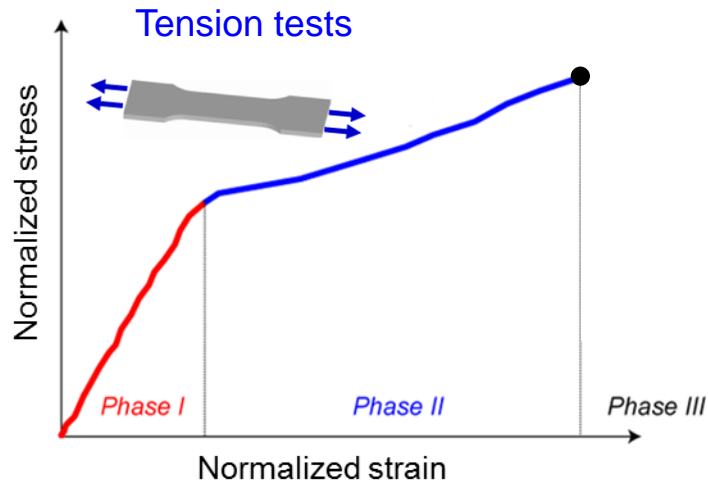
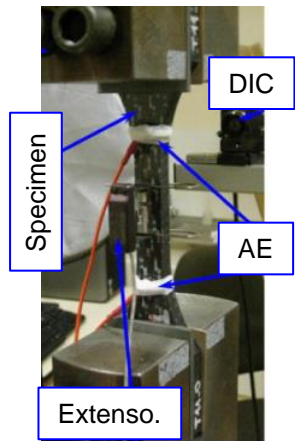
Computational strategies



Implementation in FE codes

- In-house code Zset
- Commercial code Abaqus
- Commercial code Samcef

Damage and failure scenario of 3D woven composite

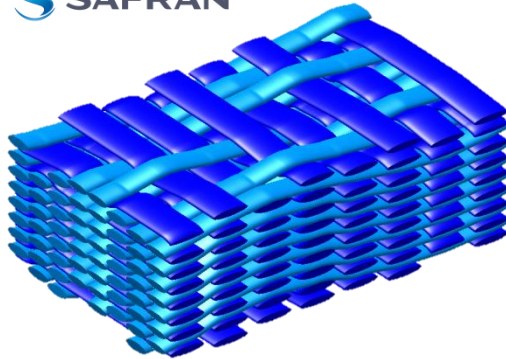


Multi-instrumented tests

- Determination of damage scenario
 - Use of different advanced techniques
 - Cross-check to \nearrow confidence in data
 - Strain, crack density, ...*
 - Complementary \rightarrow understand the material
 - Surface, volume, ...*
- Matrix damage and failure mechanisms

3D woven PMC

SAFRAN

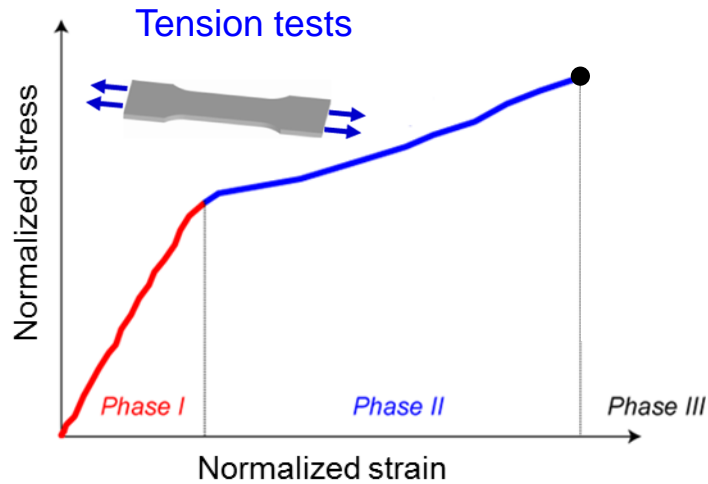
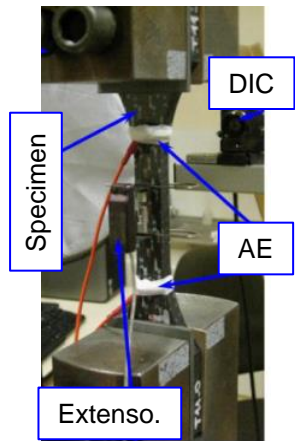


Studied material

- 3D woven composite
- Carbon / Epoxy
- Highly unbalanced 3D woven
- Large RVE

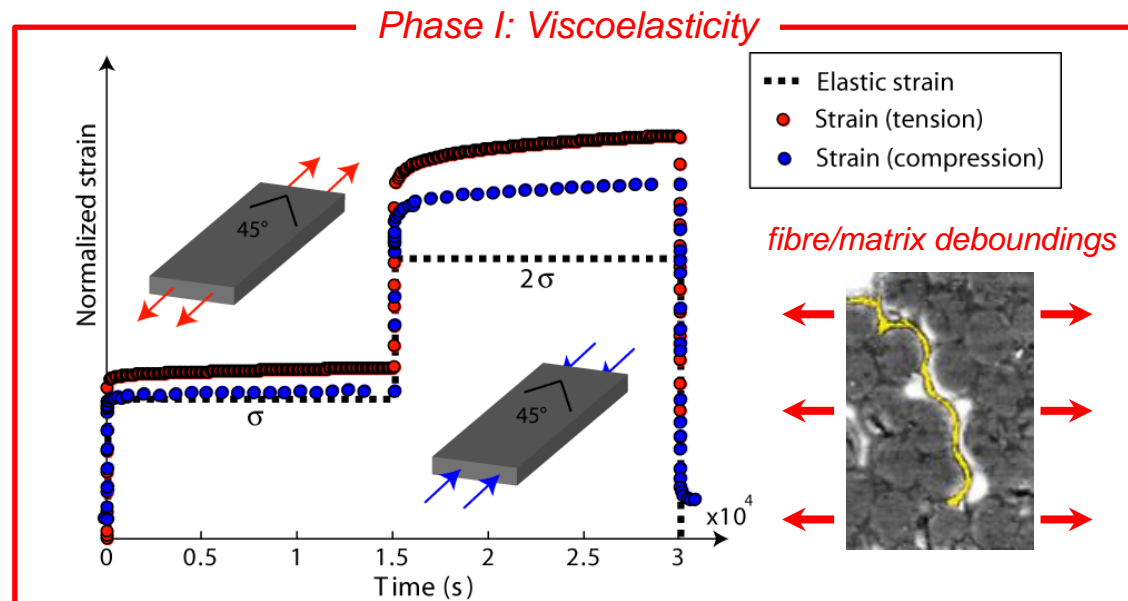
Objective: Determination of the damage scenario for different loadings

Damage and failure scenario of 3D woven composite

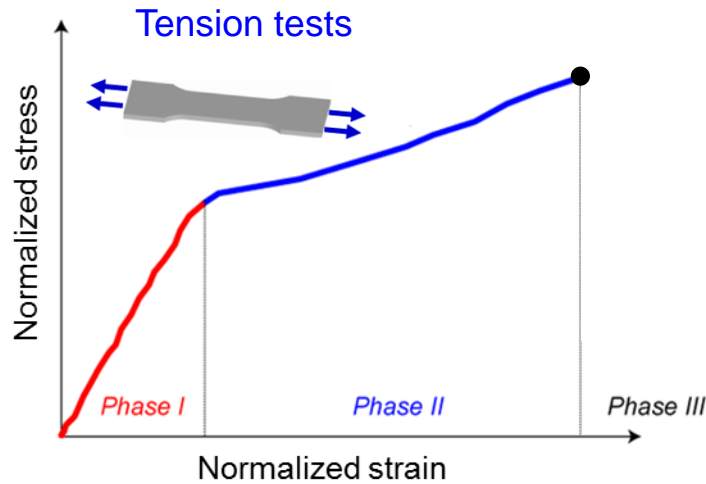
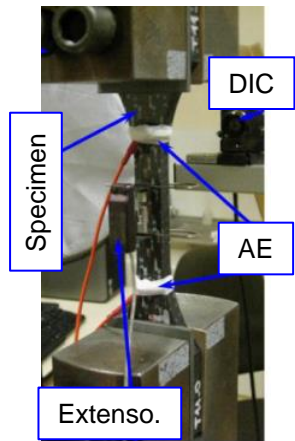


Multi-instrumented tests

- Determination of damage scenario
 - Use of different advanced techniques
 - Cross-check to \nearrow confidence in data
 - Strain, crack density, ...*
 - Complementary \rightarrow understand the material
 - Surface, volume, ...*
- Matrix damage and failure mechanisms



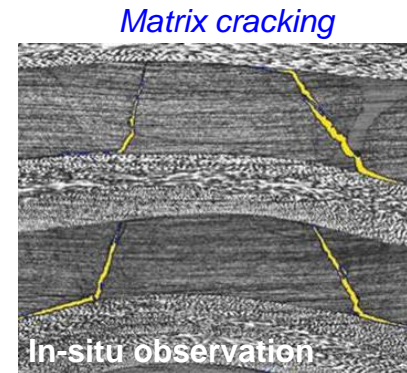
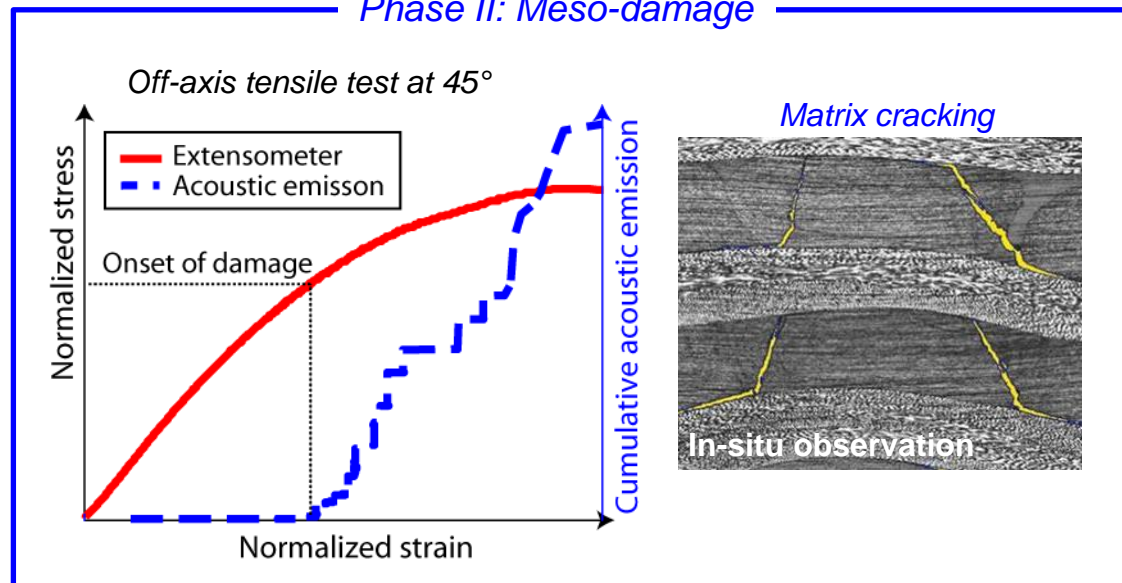
Damage and failure scenario of 3D woven composite



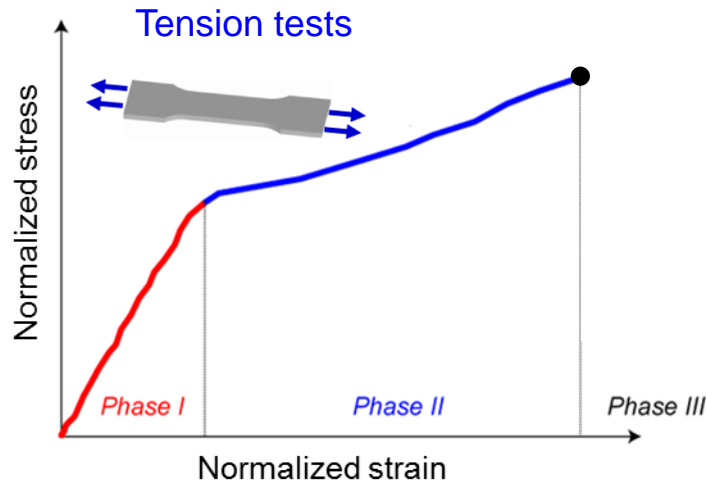
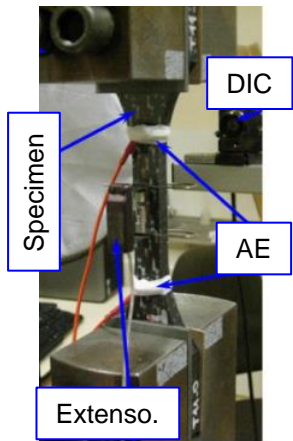
Multi-instrumented tests

- Determination of damage scenario
 - Use of different advanced techniques
 - Cross-check to \nearrow confidence in data
 - Strain, crack density, ...*
 - Complementary \rightarrow understand the material
 - Surface, volume, ...*
 - Matrix damage and failure mechanisms

Phase II: Meso-damage



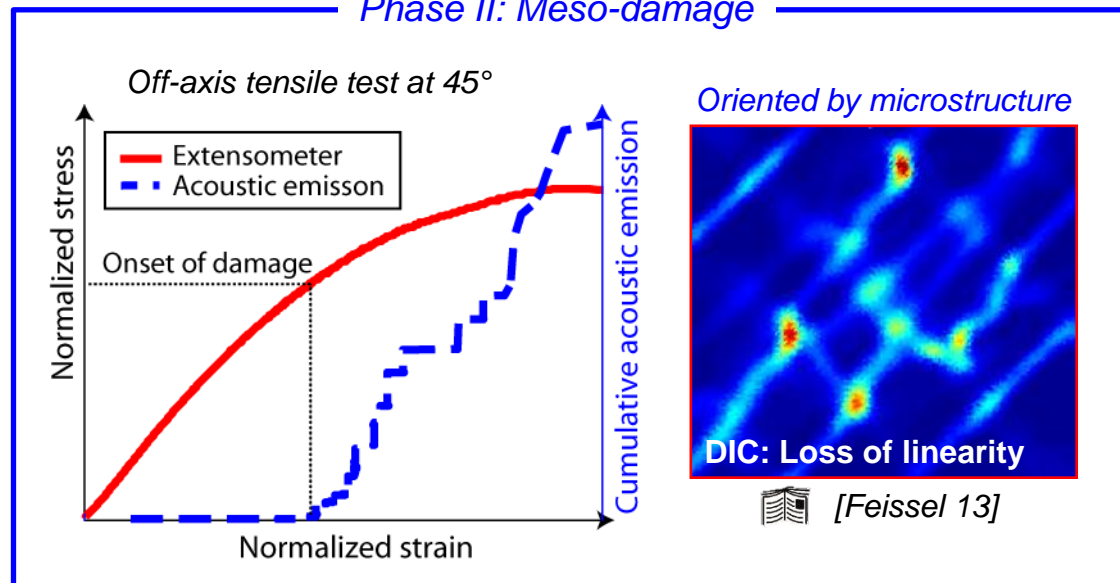
Damage and failure scenario of 3D woven composite



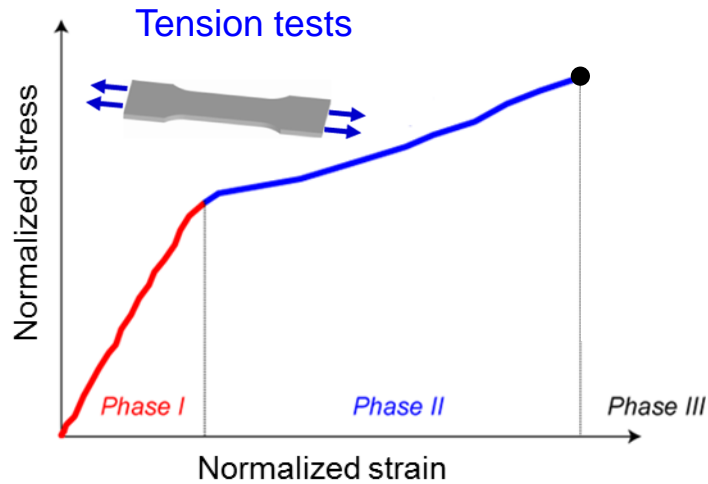
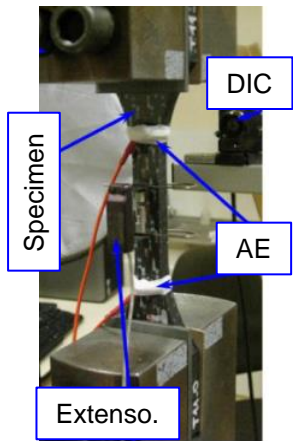
Multi-instrumented tests

- Determination of damage scenario
 - Use of different advanced techniques
 - Cross-check to \nearrow confidence in data
 - Strain, crack density, ...*
 - Complementary \rightarrow understand the material
 - Surface, volume, ...*
 - Matrix damage and failure mechanisms

Phase II: Meso-damage



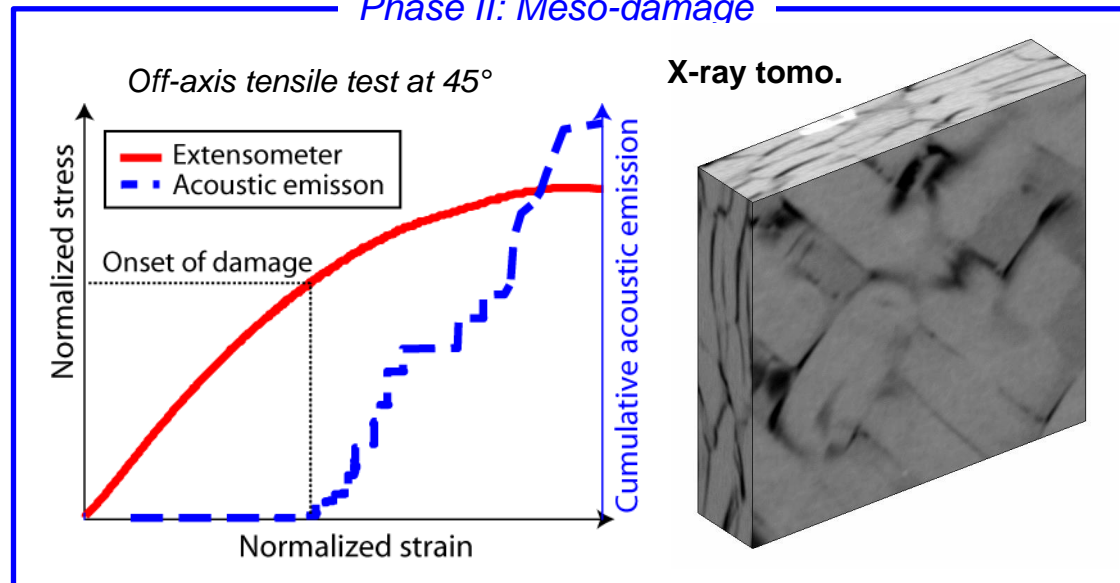
Damage and failure scenario of 3D woven composite



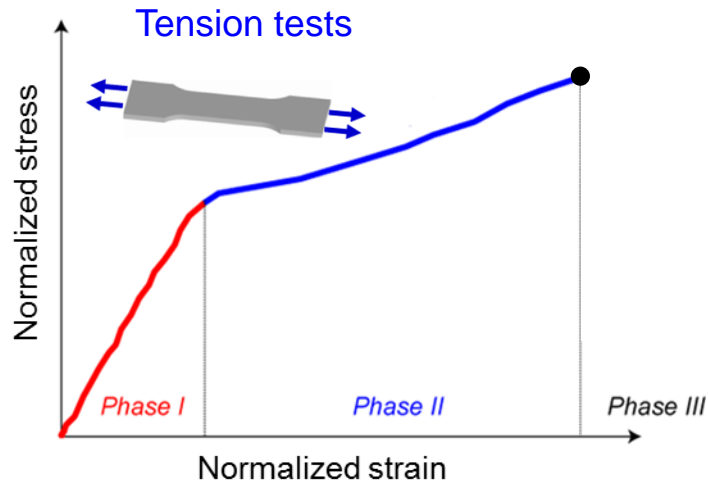
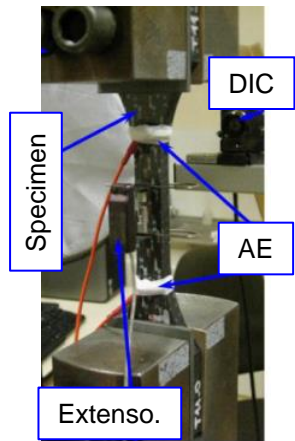
Multi-instrumented tests

- Determination of damage scenario
 - Use of different advanced techniques
 - Cross-check to \nearrow confidence in data
 - Strain, crack density, ...*
 - Complementary \rightarrow understand the material
 - Surface, volume, ...*
 - Matrix damage and failure mechanisms

Phase II: Meso-damage



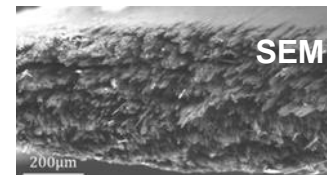
Damage and failure scenario of 3D woven composite



Multi-instrumented tests

- Determination of damage scenario
 - Use of different advanced techniques
 - Cross-check to \nearrow confidence in data
 - Strain, crack density, ...*
 - Complementary \rightarrow understand the material
 - Surface, volume, ...*
- Matrix damage and failure mechanisms

Phase III: failure mode



Failure pattern
of weft yarn

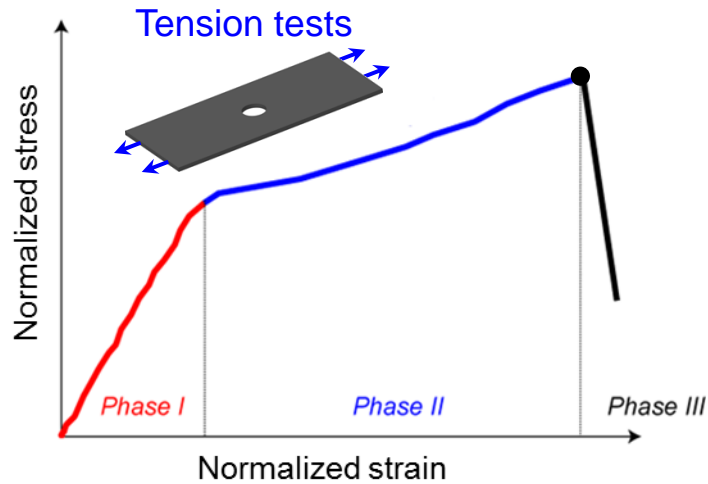
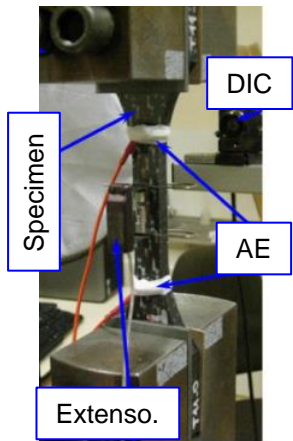


Off-axis tensile test at 45°



Failure of
fibres yarn

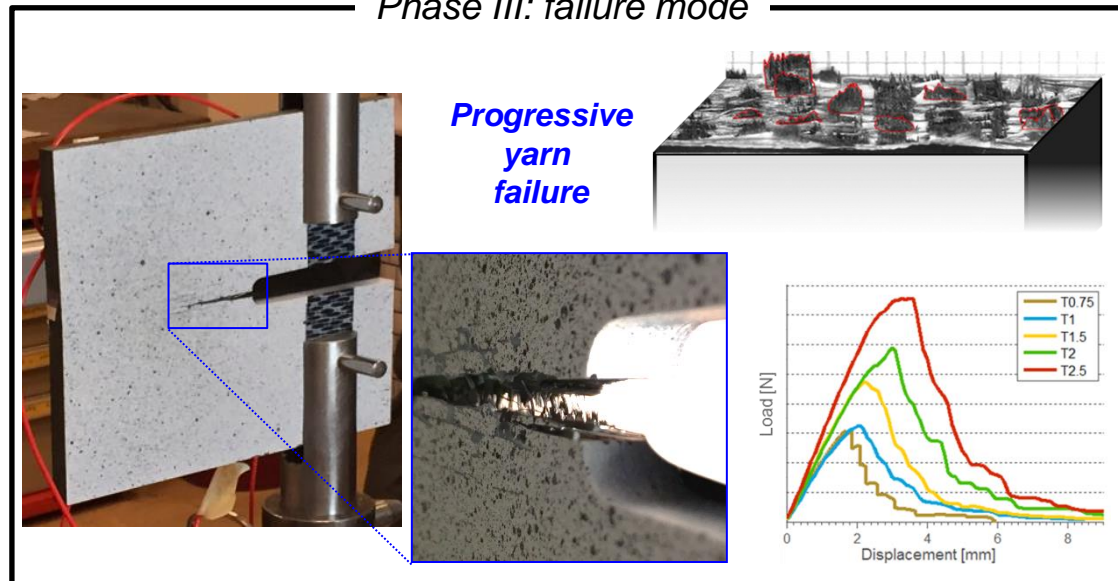
Damage and failure scenario of 3D woven composite

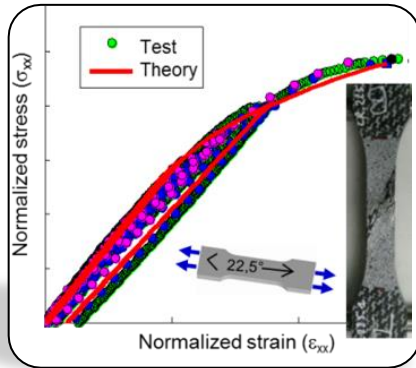


Multi-instrumented tests

- Determination of damage scenario
 - Use of different advanced techniques
 - Cross-check to \nearrow confidence in data
 - Strain, crack density, ...*
 - Complementary \rightarrow understand the material
 - Surface, volume, ...*
 - Matrix damage and failure mechanisms

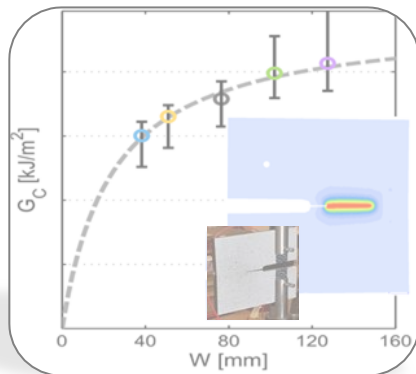
Phase III: failure mode





Damage and failure model for elementary coupons

- Comprehension of the damage and failure mechanisms
- Proposition of a macroscopic damage and failure model
- Validation through comparisons with coupon tests



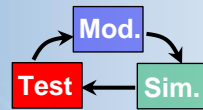
Strength of composite structures with singularities

- Experimental study on progressive yarn failures
- Modelling of fibre yarn failure – physical key quantities
- Implementation of a softening behaviour in a FE code

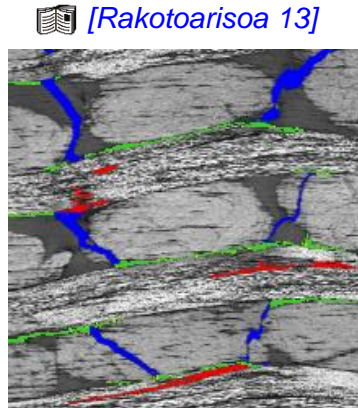
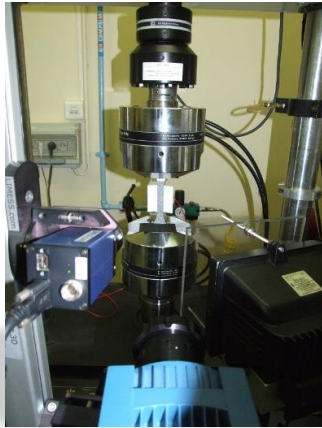
**Conclusions
Perspectives**

Advantages and limitations of failure approach
Identification protocol – Validation tests

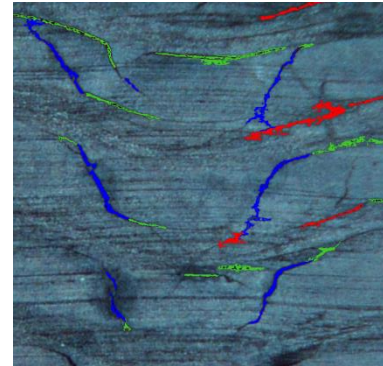
Experimental study of damage mechanisms



static



[Henry 13]



Fatigue



DIC

Video

Analysis of different damage mechanisms

Static and fatigue tests

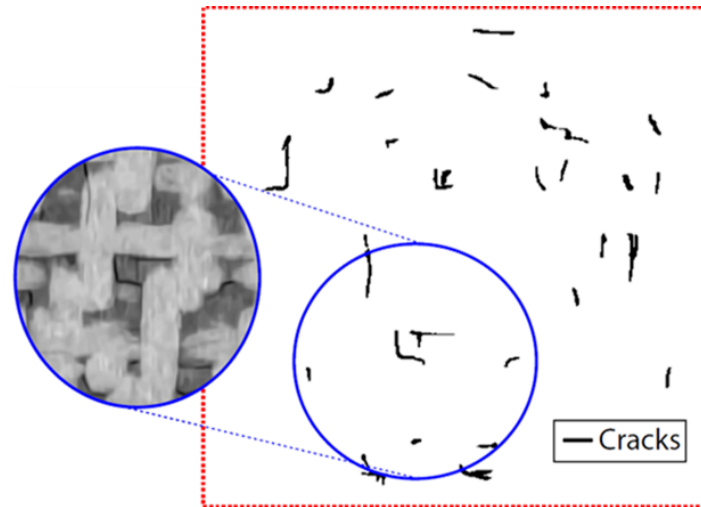
- Diffuse damage due to meso. architecture
- Similar damage for static and fatigue loadings

Impact tests (≈drop tools)

- Diffuse damage oriented by microstructure
- No large delamination cracks as in laminates

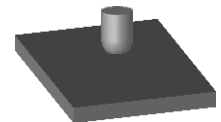
➔ Continuum damage models are relevant

[Elias16]



X-Ray tomography

Impact



Onera Damage and Failure Model for PMC

$$\underline{\underline{\sigma}} = \underline{\underline{C}}^{eff} : (\underline{\underline{\varepsilon}} - \underline{\underline{\varepsilon}}^{th} - \underline{\underline{\varepsilon}}^{ve} - \underline{\underline{\varepsilon}}^0) - \underline{\underline{C}}^0 : (\underline{\underline{\varepsilon}}^r + \underline{\underline{\varepsilon}}^s - \underline{\underline{\varepsilon}}^0)$$

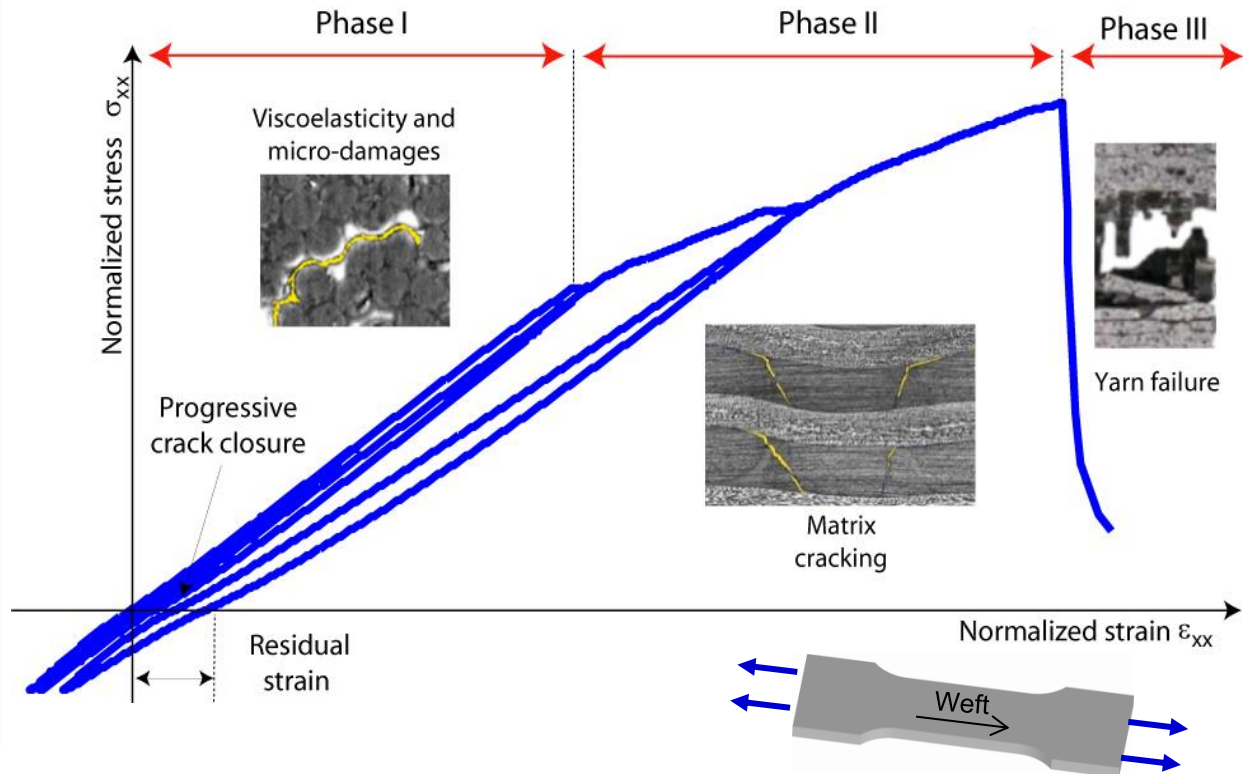
with the effective compliance $\underline{\underline{C}}^{eff} = (\underline{\underline{S}}^{eff})^{-1} = (\underline{\underline{S}}^0 + \Delta\underline{\underline{S}}^m + \Delta\underline{\underline{S}}^f)^{-1}$



[Marcin 10]
[Rakotoarisoa 13]
[Hurmane 15]
[Elias 15]

Key points

- At the macroscopic scale
- Thermodynamically consistent
- Viscoelasticity of the matrix
- Matrix damages
 - Oriented by microstructure
 - Coupling between damages
 - Stored and residual strains
- Failure of the fibre yarns
 - Oriented by microstructure
 - Softening behaviour



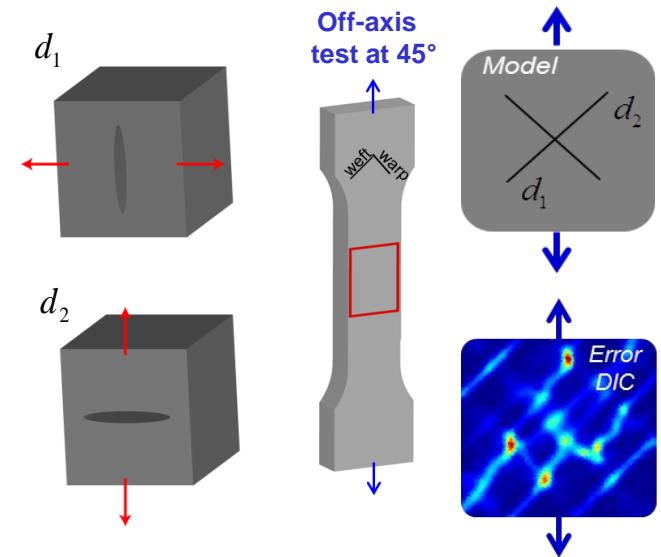
In-plane damage mechanisms

Voigt notation

- Damage oriented by architecture (2 scalar variables)
- 2 driving forces for in-plane damages

$$\begin{cases} y_1 = \frac{1}{2} \left(\varepsilon_1^{d_1^+} : C_{11}^0 : \varepsilon_1^{d_1^+} + a_{16} \varepsilon_6^{d_1^+} : C_{66}^0 : \varepsilon_6^{d_1^+} + a_{15} \varepsilon_5^{d_1^+} : C_{55}^0 : \varepsilon_5^{d_1^+} \right) \\ y_2 = \frac{1}{2} \left(\varepsilon_2^{d_2^+} : C_{22}^0 : \varepsilon_2^{d_2^+} + a_{26} \varepsilon_6^{d_2^+} : C_{66}^0 : \varepsilon_6^{d_2^+} + a_{24} \varepsilon_4^{d_2^+} : C_{44}^0 : \varepsilon_4^{d_2^+} \right) \end{cases}$$

- ε^+ used to improve predictions of onset of damage
 - Reinforcement for combined shear / compression loading



Out-of-plane damage mechanism

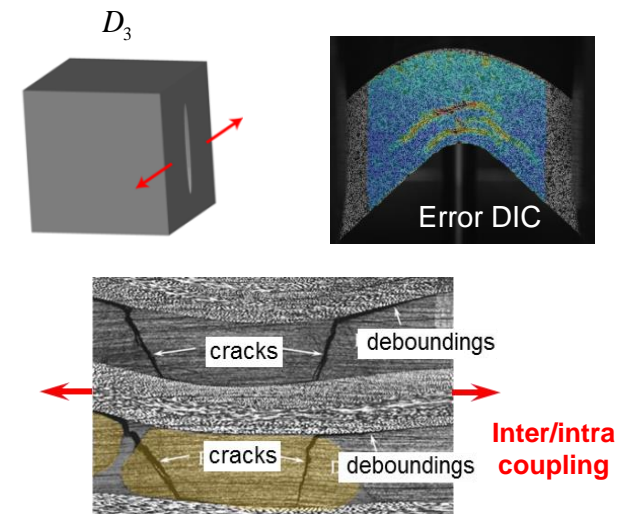
Voigt notation

- 2 elementary thermo-dynamical forces

$$y_3 = y_3^p + y_3^{php}$$

$$\begin{cases} y_3^p = \frac{1}{2} \left(\varepsilon_3^{D_3^+} : C_{33}^0 : \varepsilon_3^{D_3^+} + a_{34} \varepsilon_4^{D_3^+} : C_{44}^0 : \varepsilon_4^{D_3^+} + a_{35} \varepsilon_5^{D_3^+} : C_{55}^0 : \varepsilon_5^{D_3^+} \right) \\ y_3^{php} = \frac{1}{2} \left(c_{31} \langle \varepsilon_1 \rangle_+^2 + c_{32} \langle \varepsilon_2 \rangle_+^2 + c_{36} \varepsilon_6^2 \right) \end{cases}$$

- Coupling between in-plane and out-of-plane loading



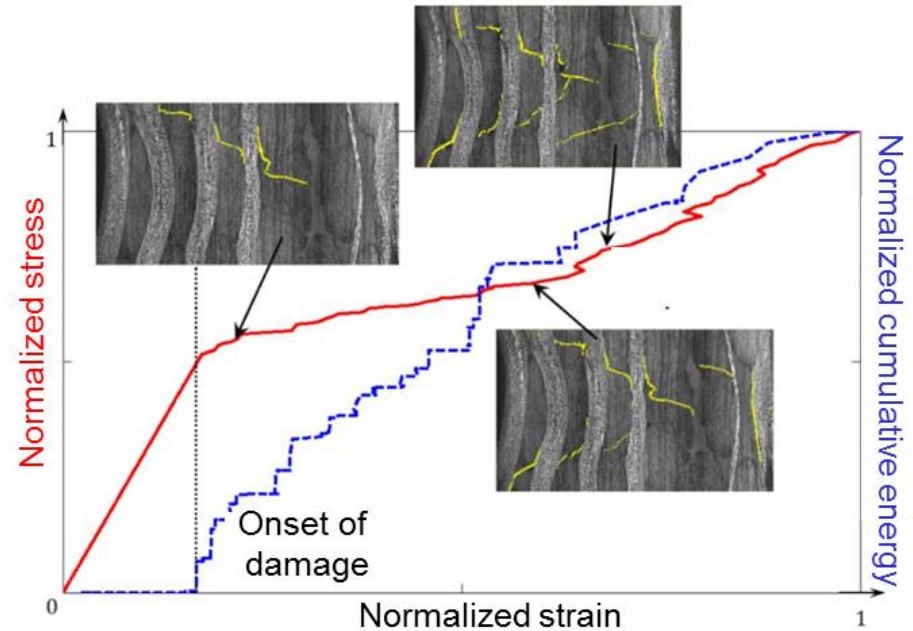
Damage evolution laws

Damage evolution laws

- Onset of damage y_0
- Saturation of damage d_c
- Evolution parameters (y_0, p)

$$d_i = d_{c_i} \cdot \left(1 - \exp \left(- \left(\frac{\langle \sqrt{y_i} - \sqrt{y_{0_i}} \rangle_+}{\sqrt{y_{c_i}}} \right)^{p_i} \right) \right)$$

- Damage can only grow $\dot{d}_i \geq 0$



Anisotropic effect tensors

Influence on the effective compliance

$$\Delta \underline{\underline{S}}^m = \sum_i d_i \underline{\underline{H}}_i$$

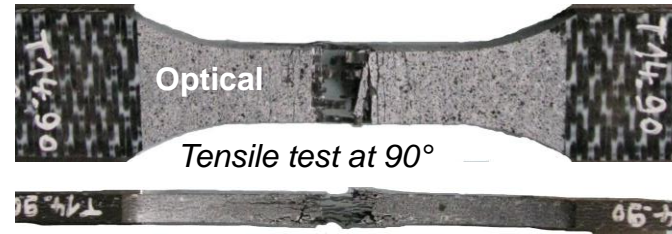
- Depend on the elastic properties
- Determined thanks to micromechanical approach [Laws & Sih 77]

The diagram shows a 3D cube with a vertical crack along the x_1 axis. Red arrows indicate the direction of applied stress. The anisotropic effect tensor $\underline{\underline{H}}_1^+$ is given by:

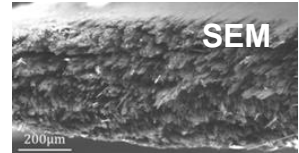
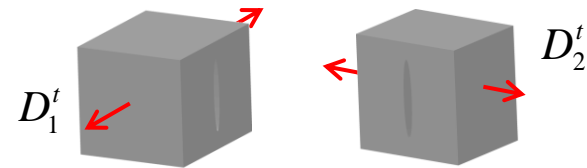
$$\underline{\underline{H}}_1^+ = \begin{pmatrix} h_{11}^{1+} S_{11}^0 & 0 & 0 & 0 & 0 & 0 \\ 0 & 0 & 0 & 0 & 0 & 0 \\ 0 & 0 & 0 & 0 & 0 & 0 \\ 0 & 0 & 0 & 0 & 0 & 0 \\ sym. & & & h_{55}^{1+} S_{55}^0 & 0 & \\ & & & & & h_{66}^{1+} S_{66}^0 \end{pmatrix}$$

Tension failure of fibre yarns

- Failure cracks are oriented by the microstructure (failure of fibre yarns)
- 2 scalar failure variables (D_1^t, D_2^t)
 - Driving forces $y_1^{D^+} = \frac{1}{2} C_{11}^0 \langle \varepsilon_1 \rangle_+^2$ and $y_2^{D^+} = \frac{1}{2} C_{22}^0 \langle \varepsilon_2 \rangle_+^2$



[Hurmane 15]

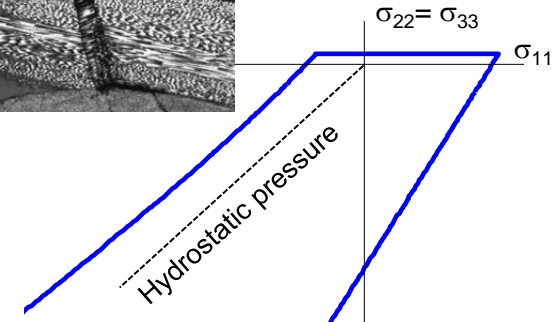
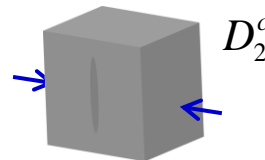
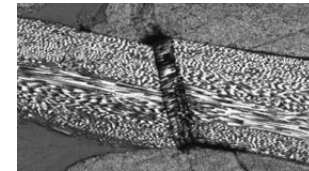
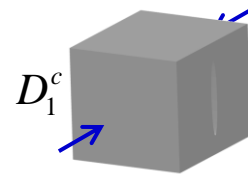


Compression failure of fibre yarns

- Failure cracks are oriented by the microstructure (orientation of fibre yarns)
- 2 scalar failure variables (D_1^c, D_2^c)
 - Driving forces
$$\begin{cases} y_1^{D^-} = \sqrt{\langle \sigma_1 - \sigma_3 \rangle_+^2 + a_1^t \tau_{13}^2} \\ y_2^{D^-} = \sqrt{\langle \sigma_2 - \sigma_3 \rangle_+^2 + a_2^t \tau_{23}^2} \end{cases}$$
- Influence of the hydrostatic pressure
 - No possible failure if $\sigma_{11} = \sigma_{22} = \sigma_{33}$ compression
- Influence of the out-of-plane shears



[Elias 15]



Implementation in FE codes

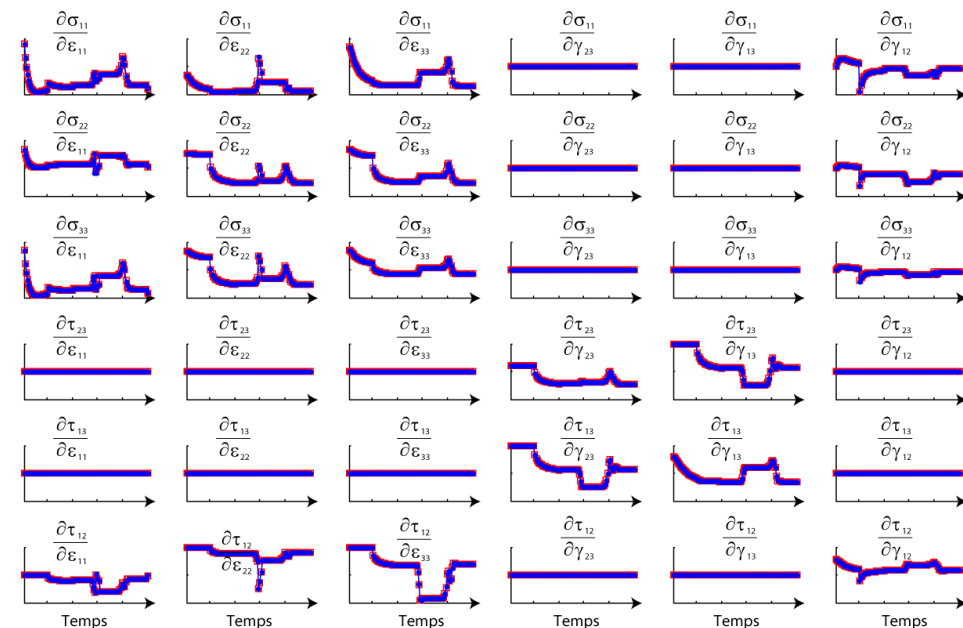
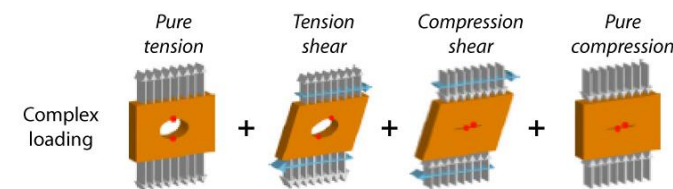
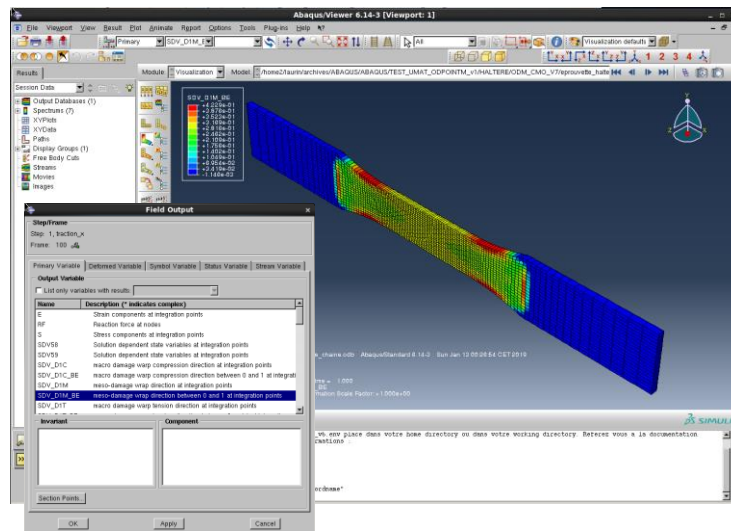
Implementation in different FE Codes

- Available in different commercial finite element codes with implicit solver



Definition of variables useful in design offices

- Proposition of driving forces and damage variables simple to analyse (evolving between 0 and 1)

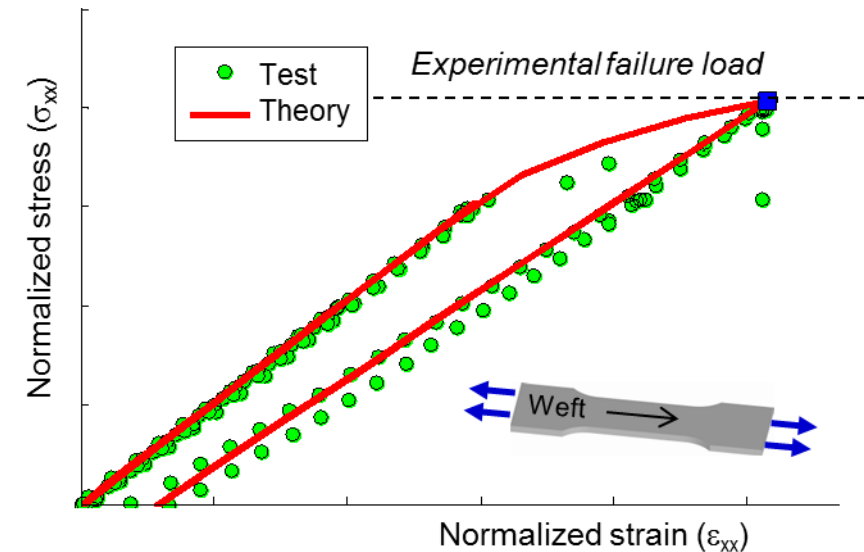
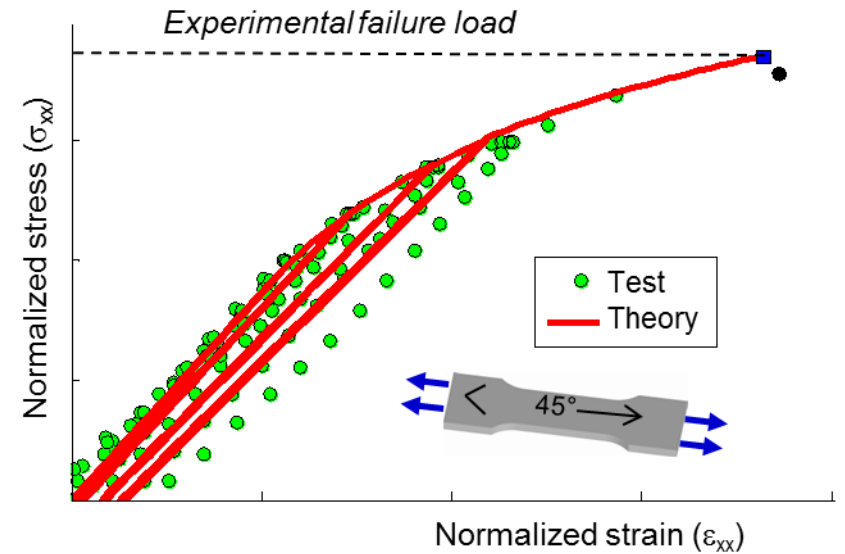
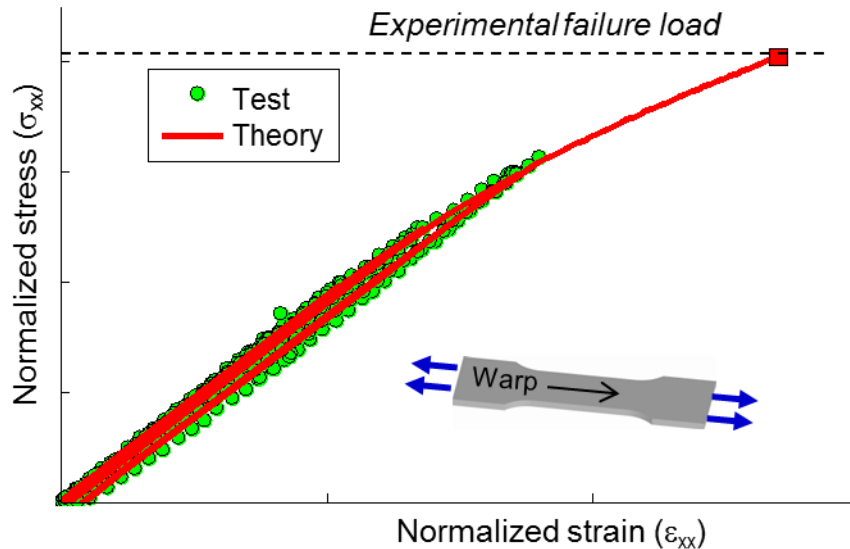


Special care to the accuracy of the consistent tangent matrix

- Validation thanks to cross-check with numerical solution on 51 test cases (perturbation method)
- Non symmetrical 4th order tensor

Conclusions

- Off-axis tensile tests at different angles
 - Multi-instrumented incremental tensile tests at 0° , 22.5° , 45° , 67.5° and 90° performed at Onera
 - [Rakotoarisoa 11], [Elias 15]
- Predictions are in good agreement with the available test results
 - Evolution of the apparent moduli, effects of crack closure, residual strain and failure predictions



Conclusions

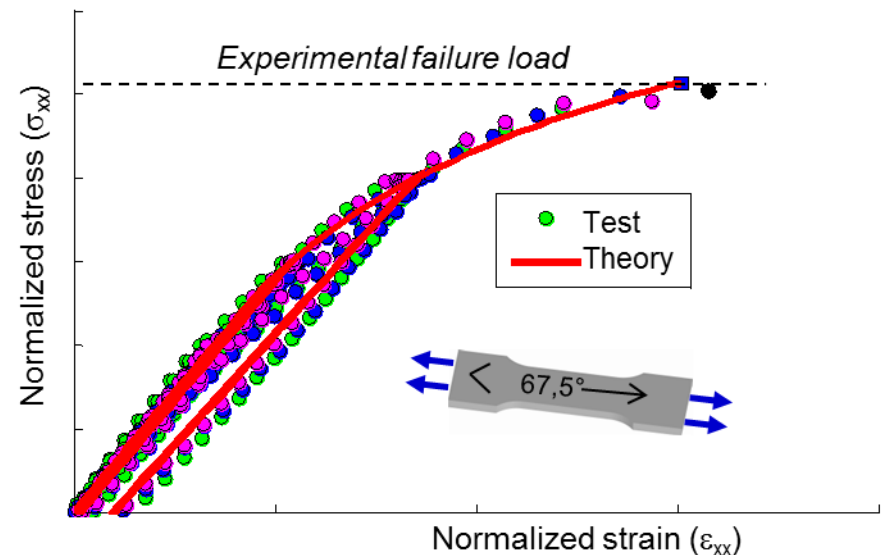
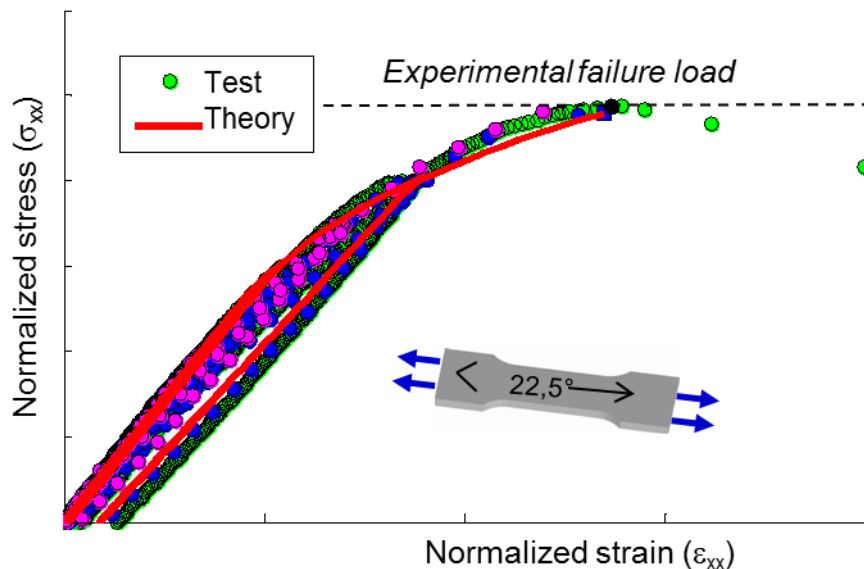
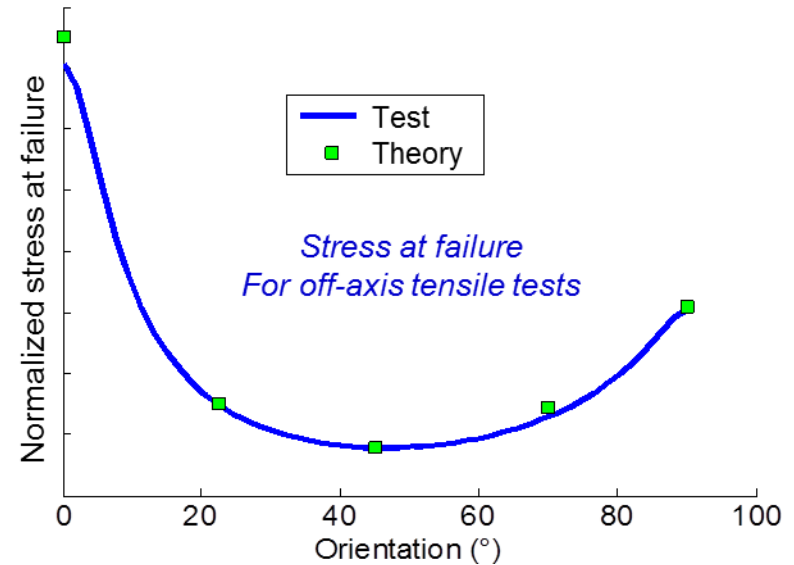
Off-axis tensile tests at different angles

- Multi-instrumented incremental tensile tests at 0° , 22.5° , 45° , 67.5° and 90° performed at Onera

[Rakotoarisoa 11], [Elias 15]

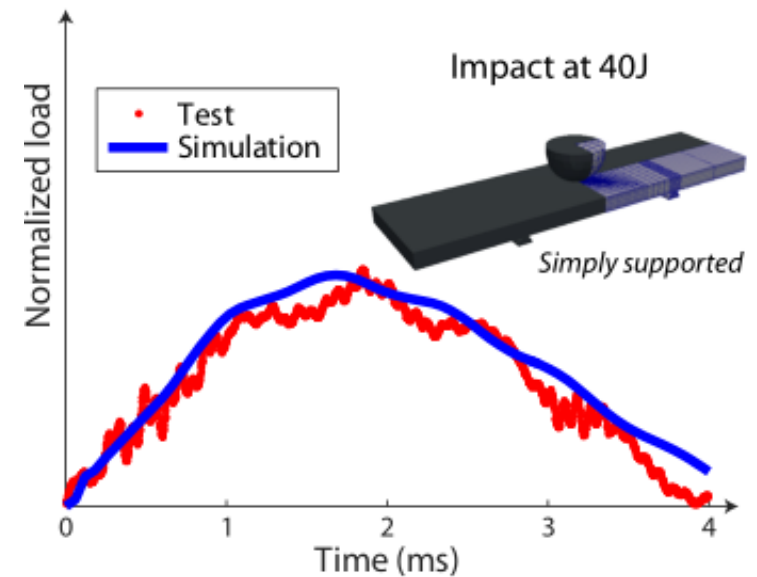
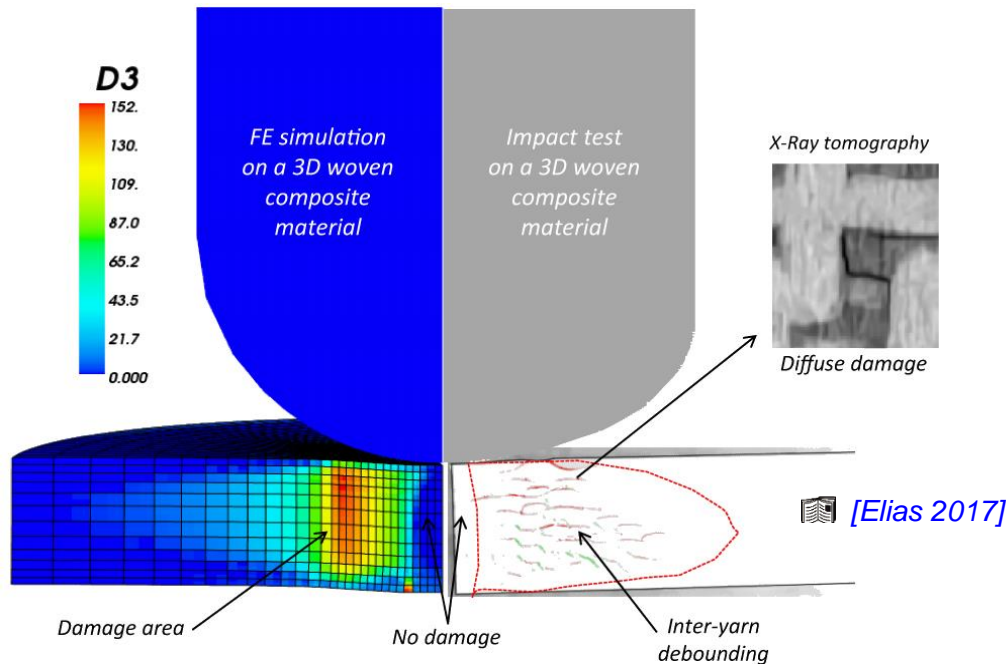
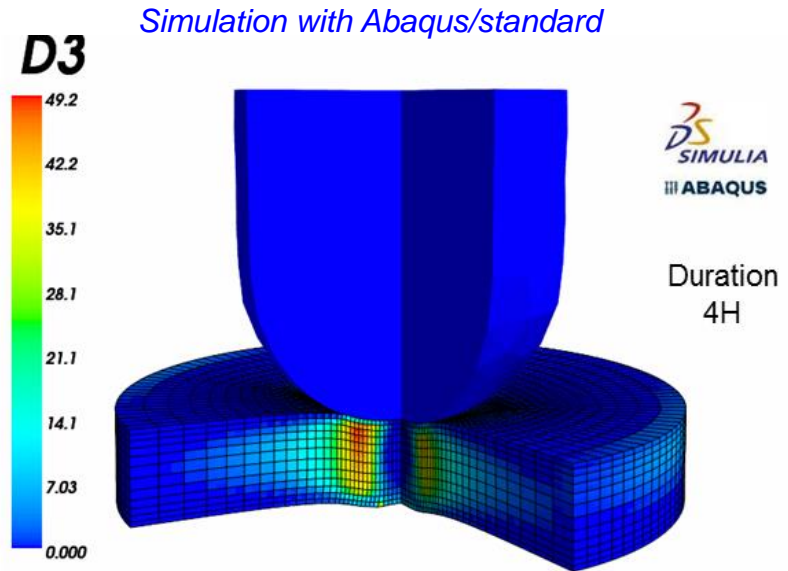
Predictions are in good agreement with the available test results

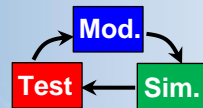
- Evolution of the apparent moduli, effects of crack closure, residual strain and failure predictions



Extension to impact problems

- 🔧 **Simulation of impact tests**
 - Simulation with abaqus/standard (*implicit solver*)
 - Robust and efficient modelling (few hours)
- 🔧 **Comparisons with test results**
 - Accurate predictions of load/time curves for different impact energies
 - Accurate estimation of damage patterns through the thickness of the specimens





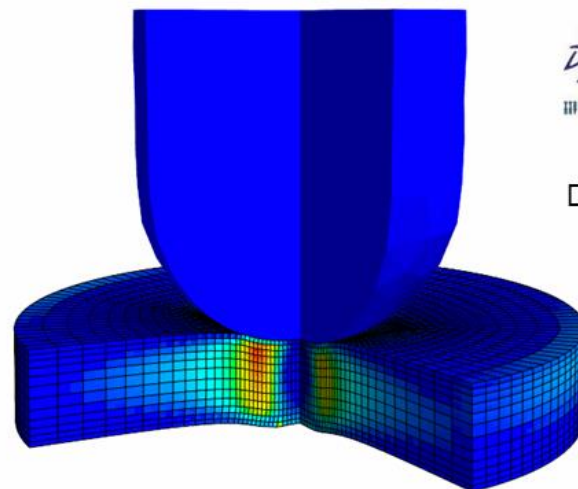
Extension to impact problems

- Simulation of impact tests
 - Simulation with abaqus/standard (*implicit solver*)
 - Robust and efficient modelling (few hours)
- Comparisons with test results
 - Accurate predictions of load/time curves for different impact energies
 - Accurate estimation of damage patterns through the thickness of the specimens

D3

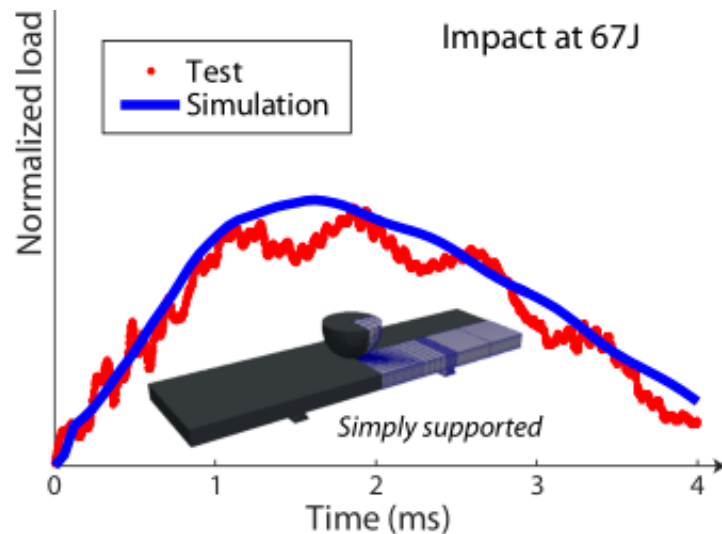
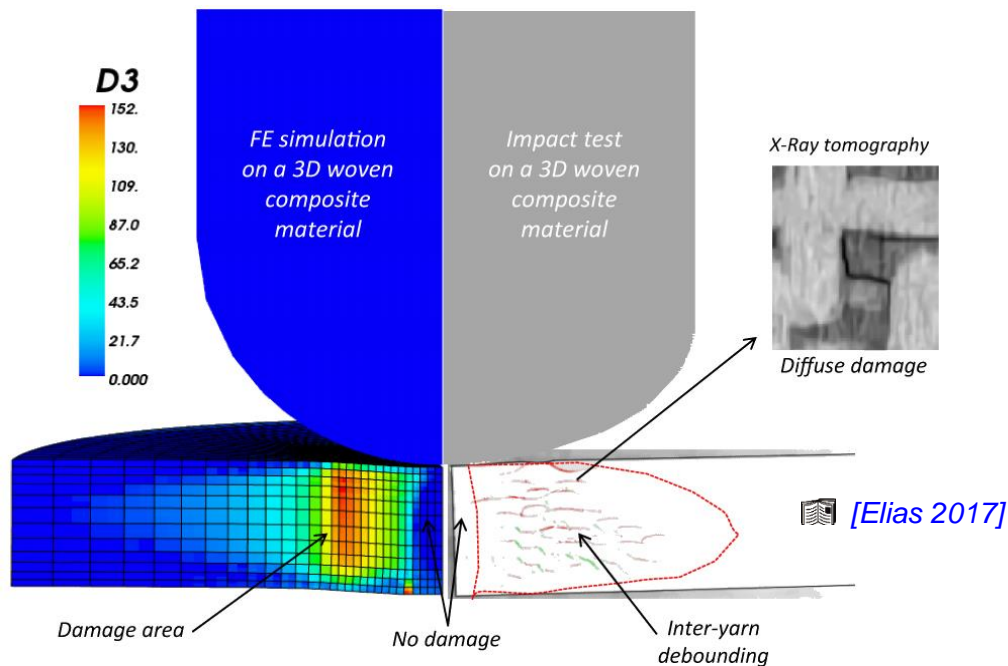


Simulation with Abaqus/standard



3
SIMULIA
ABAQUS

Duration
4H



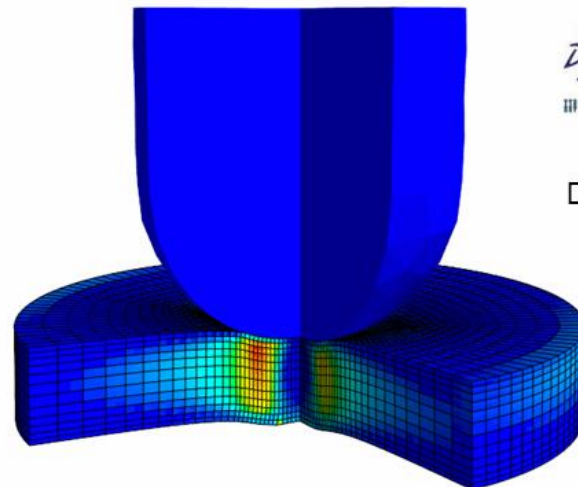
Extension to impact problems

- Simulation of impact tests
 - Simulation with abaqus/standard (*implicit solver*)
 - Robust and efficient modelling (few hours)
- Comparisons with test results
 - Accurate predictions of load/time curves for different impact energies
 - Accurate estimation of damage patterns through the thickness of the specimens

D3

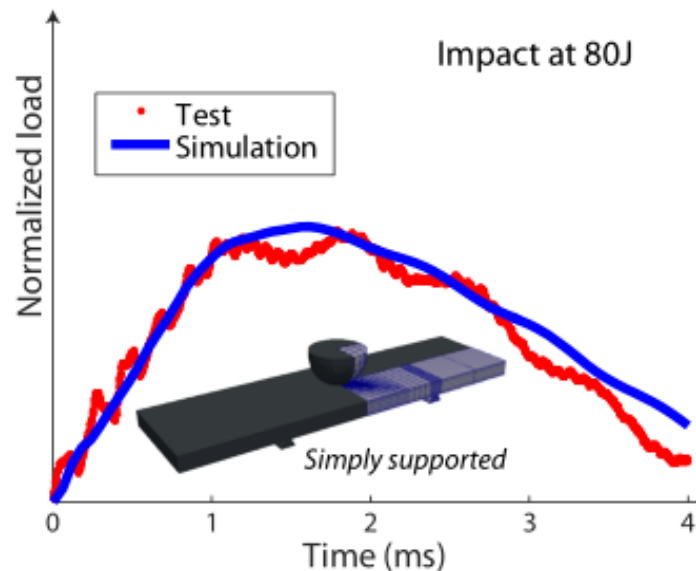
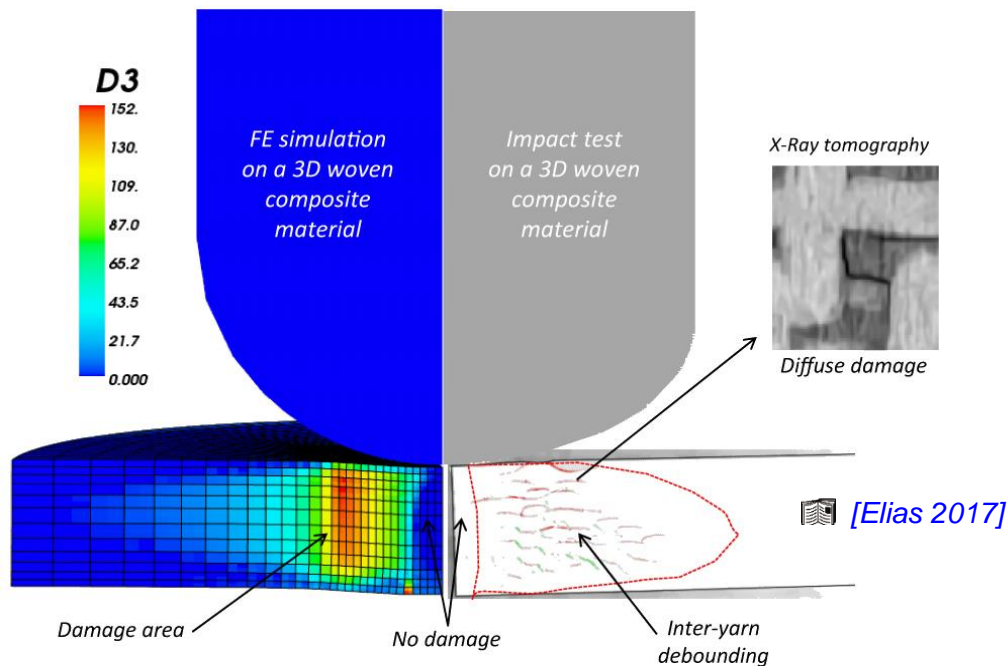


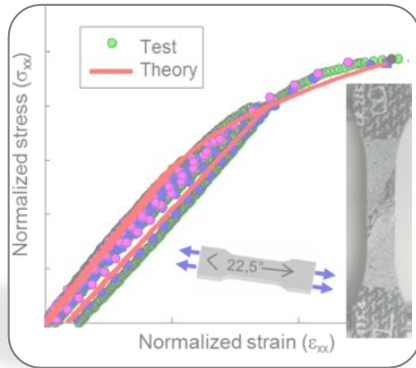
Simulation with Abaqus/standard



3D
SIMULIA
ABAQUS

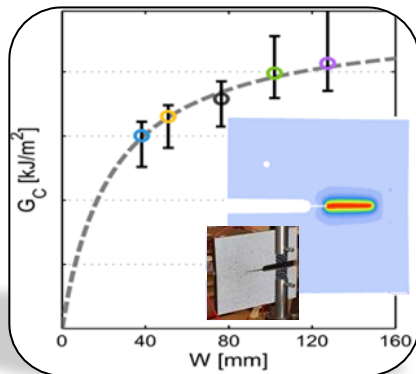
Duration
4H





Damage and failure model for elementary coupons

- Comprehension of the damage and failure mechanisms
- Proposition of a macroscopic damage and failure model
- Validation through comparisons with tests



Strength of composite structures with singularities

- Experimental study on progressive yarn failures
- Modelling of fibre yarn failure – physical key quantities
- Implementation of a softening behaviour in a FE code

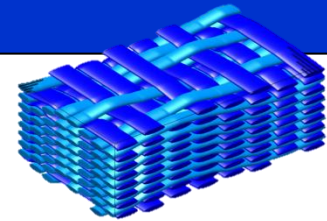
**Conclusions
Perspectives**

Advantages and limitations of failure approach
Identification protocol – Validation tests

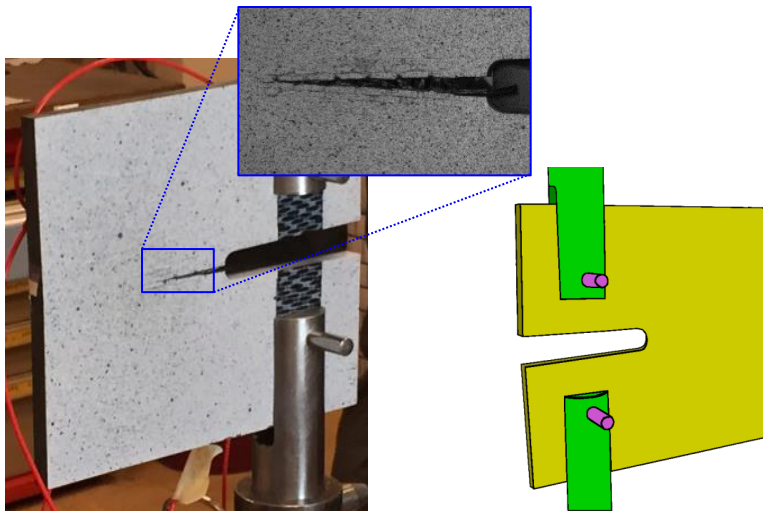
Presentation of the test campaign

Test configurations with stable crack propagation

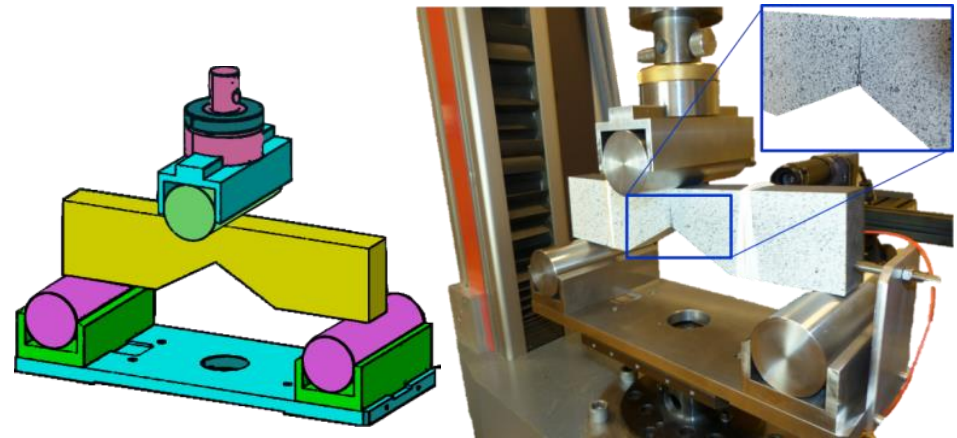
- 3D highly unbalanced woven material tested in the weft direction
- Identification of the *critical energy release rate* G_c for fibre yarn failure
 - Compact Tension test (CT) [ASTM E1922-04], [Pinho 06], [Laffan10], [Bergan 16]
 - Single Edge Notched Beam (SENB) [ASTM 5045-99]
- Design of specimens with specificities of 3D woven composites [Blanco 14]



Size effect for CT specimens (5 different sizes with a constant thickness)



Configuration of the standard CT test

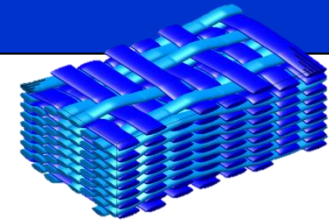


Configuration of the standard SENB test

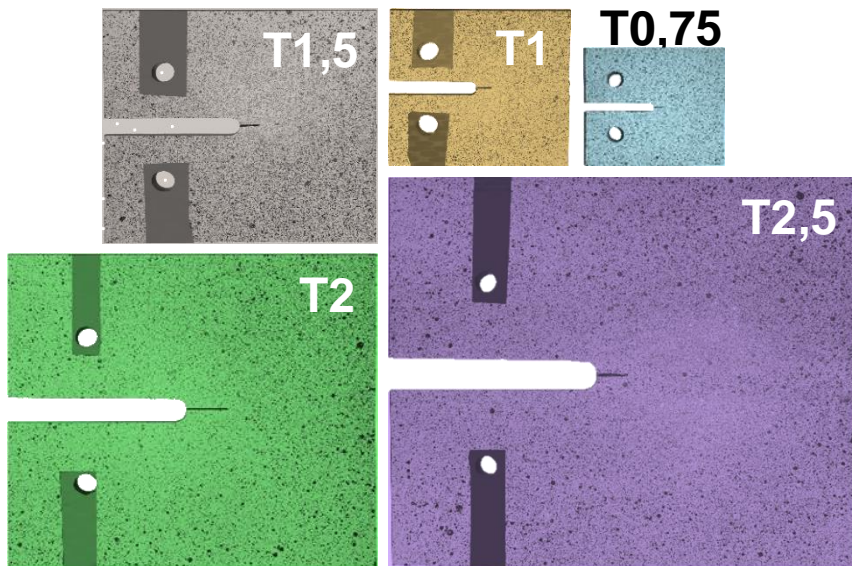
Presentation of the test campaign

Test configurations with stable crack propagation

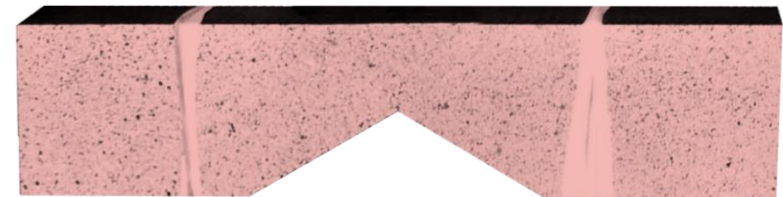
- 3D highly unbalanced woven material tested in the weft direction
- Identification of the *critical energy release rate* G_c for fibre yarn failure
 - Compact Tension test (CT) [ASTM E1922-04], [Pinho 06], [Laffan10], [Bergan 16]
 - Single Edge Notched Beam (SENB) [ASTM 5045-99]
- Design of specimens with specificities of 3D woven composites [Blanco 14]



Size effect for CT specimens (5 different sizes with a constant thickness)



Homothetic CT specimens



SENB specimen

Crack propagation

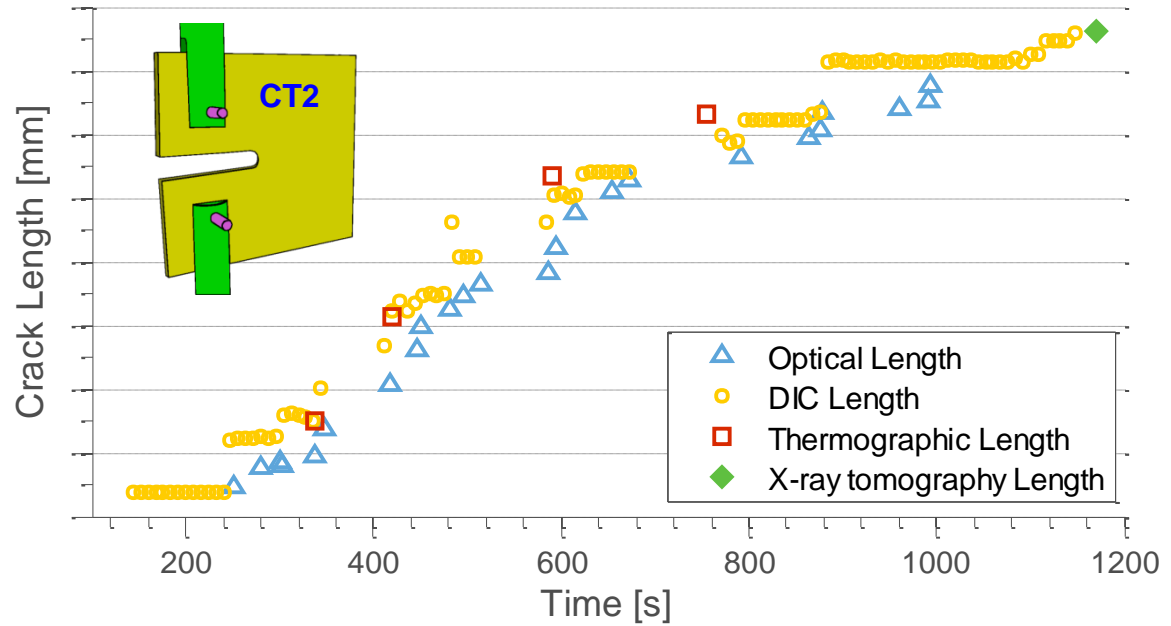
Different measurement techniques

- Optical tracking (*grey level gradient*)
- DIC tracking (*discontinuity disp. field*)
- IR thermography (*heating crack*)
- X-Ray tomography (*ex and in-situ*)

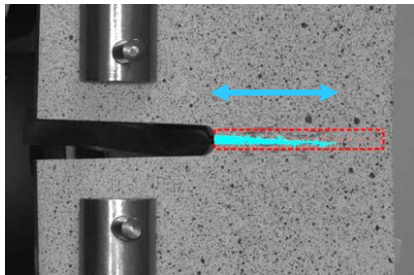
Different measurement techniques

- Cross-check to \nearrow confidence
- Complementary technique

Surface, volume, ...

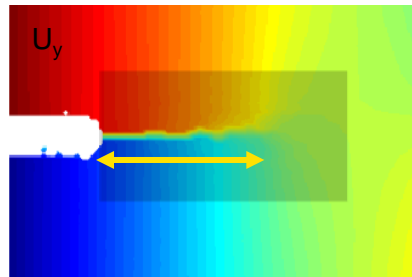


Optical tracking



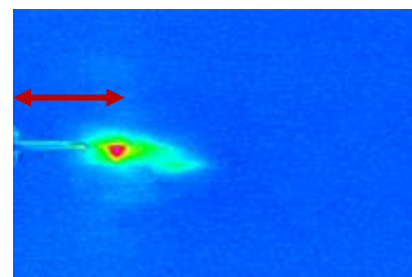
[Pack 17]
[Panin 17]

DIC tracking



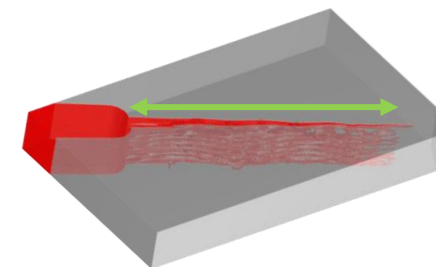
[Lopez-Crespo 08]
[Vanlanduit 09]
[Catalanotti 10]

IR Thermography



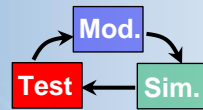
[Muller 16]
[Archer 17]

X-ray Tomography



X-Ray tomography by
Safran Aircraft Engines

Measurement of macroscopic crack propagation



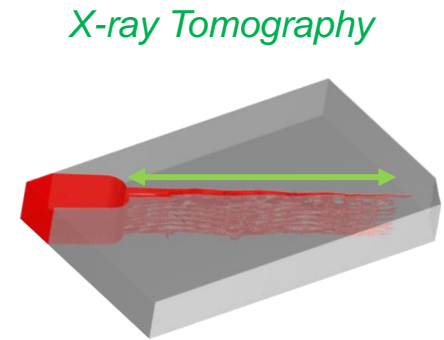
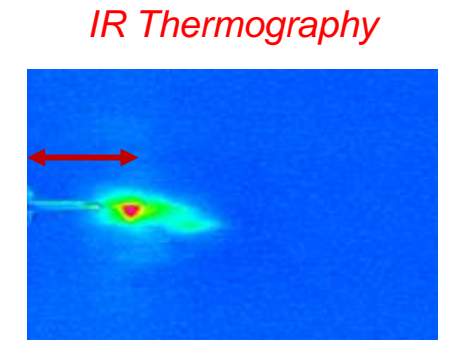
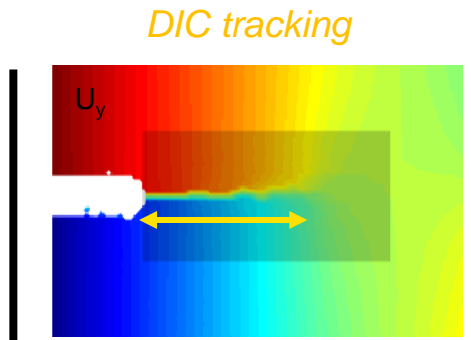
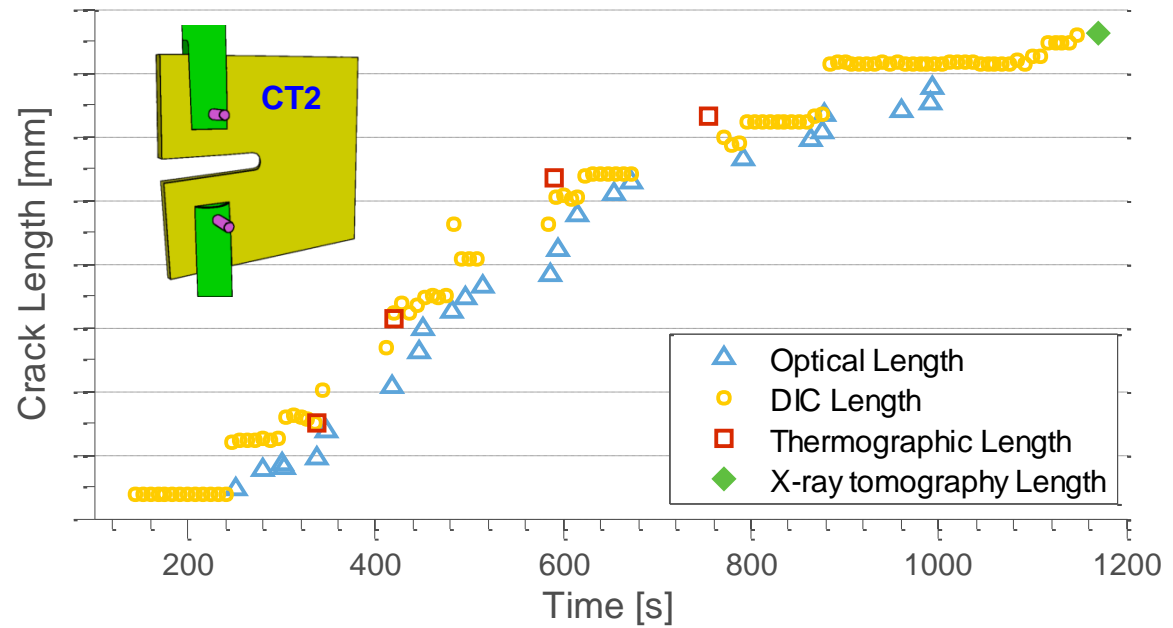
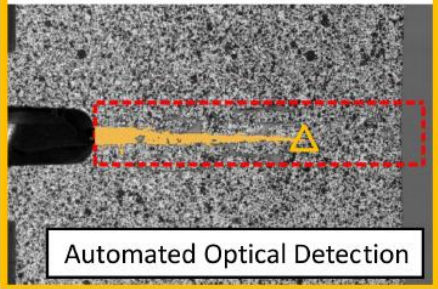
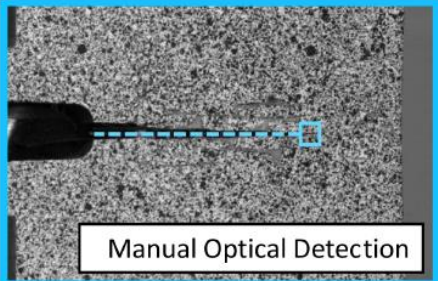
Crack propagation

Different measurement techniques

- Level gradient
- Displacement field
- Crack
- and in-situ

techniques

- Reference
- Technique



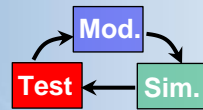
[Pack 17]
[Panin 17]

[Lopez-Crespo 08]
[Vanlanduit 09]
[Catalanotti 10]

[Muller 16]
[Archer 17]

X-Ray tomography by
Safran Aircraft Engines

Measurement of macroscopic crack propagation



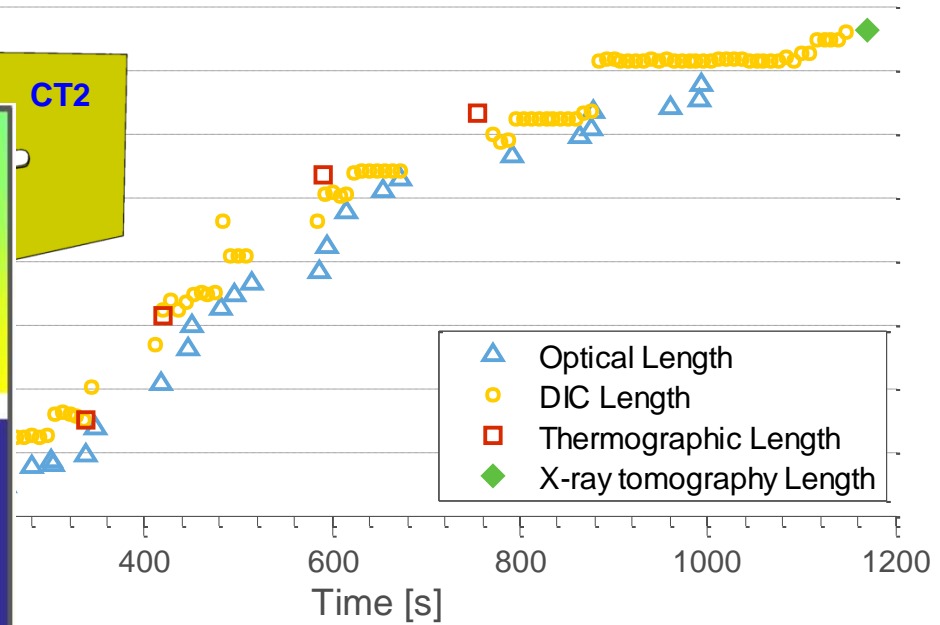
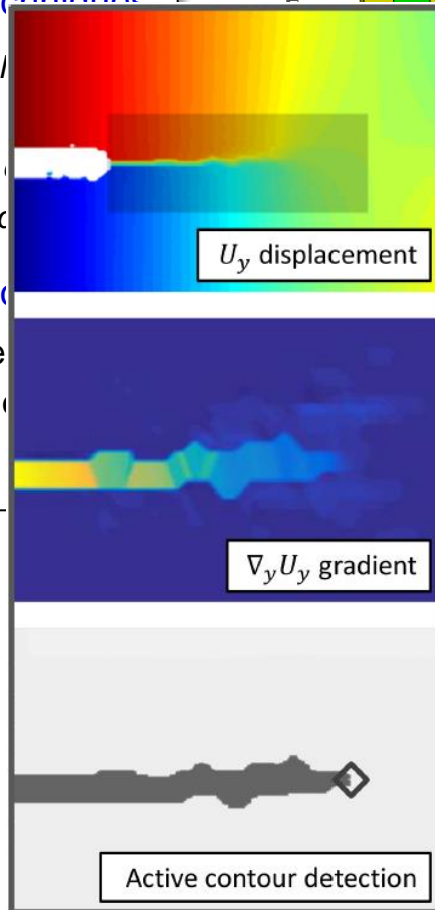
Crack propagation

Different measurement techniques

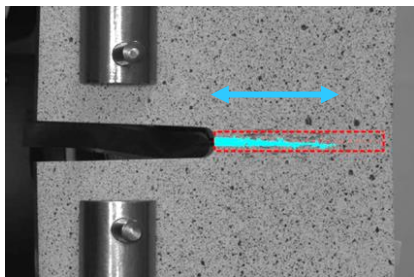
- Optical tracking (*grey level*)
- DIC tracking (*discontinuity*)
- IR thermography (*heating*)
- X-Ray tomography (*ex and*)

Different measurement techniques

- Cross-check to \nearrow confidence
- Complementary techniques
- Surface, volume, ...

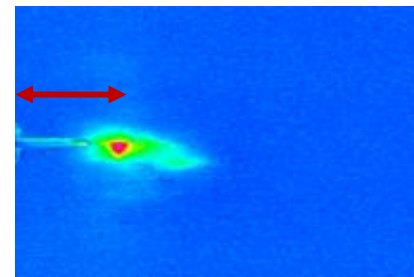


Optical tracking



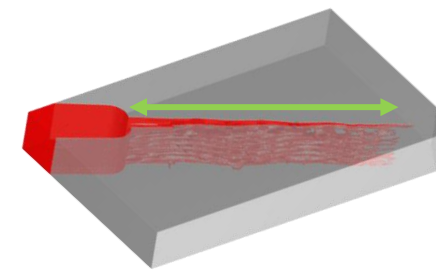
[Pack 17]
[Panin 17]

IR Thermography



[Muller 16]
[Archer 17]

X-ray Tomography

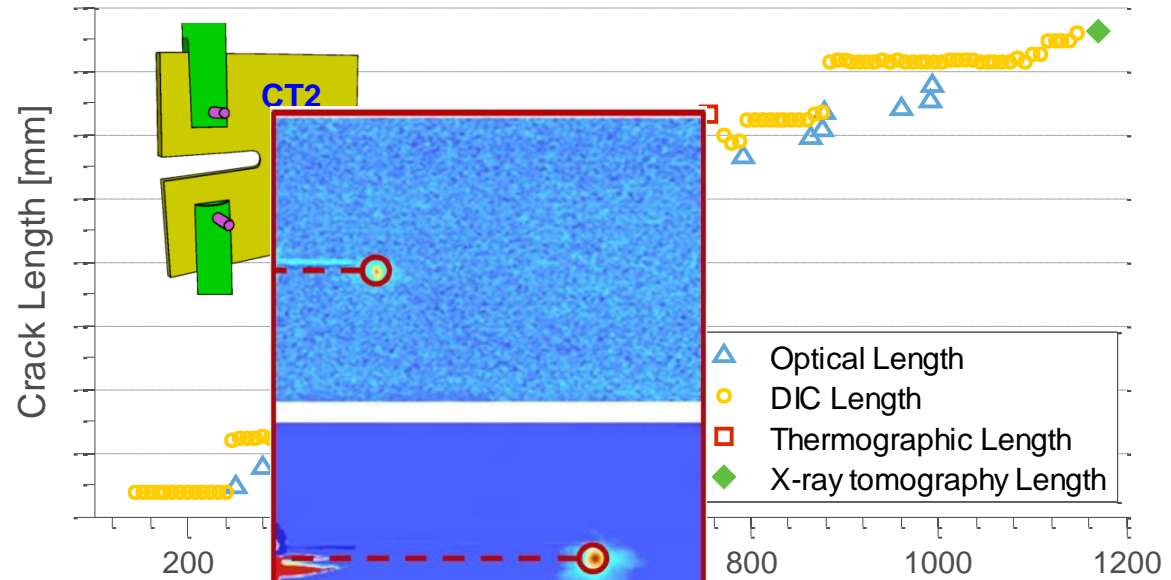


X-Ray tomography by
Safran Aircraft Engines

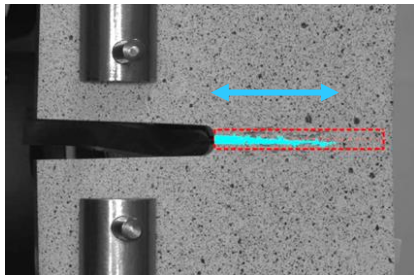
[Lopez-Crespo 08]
[Vanlanduit 09]
[Catalanotti 10]

Crack propagation

- Different measurement techniques**
 - Optical tracking (*grey level gradient*)
 - DIC tracking (*discontinuity disp. field*)
 - IR thermography (*heating crack*)
 - X-Ray tomography (*ex and in-situ*)
- Different measurement techniques**
 - Cross-check to \nearrow confidence
 - Complementary technique
 - Surface, volume, ...

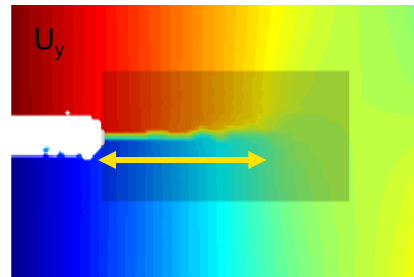


Optical tracking

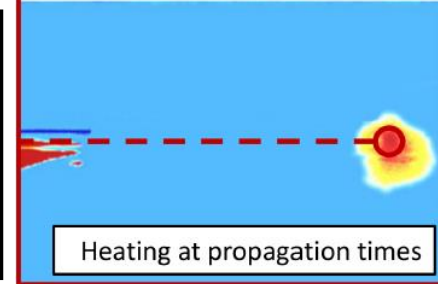


[Pack 17]
[Panin 17]

DIC tracking

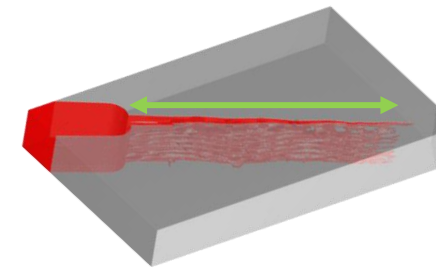


[Lopez-Crespo 08]
[Vanlanduit 09]
[Catalanotti 10]



[Muller 16]
[Archer 17]

X-ray Tomography



X-Ray tomography by
Safran Aircraft Engines

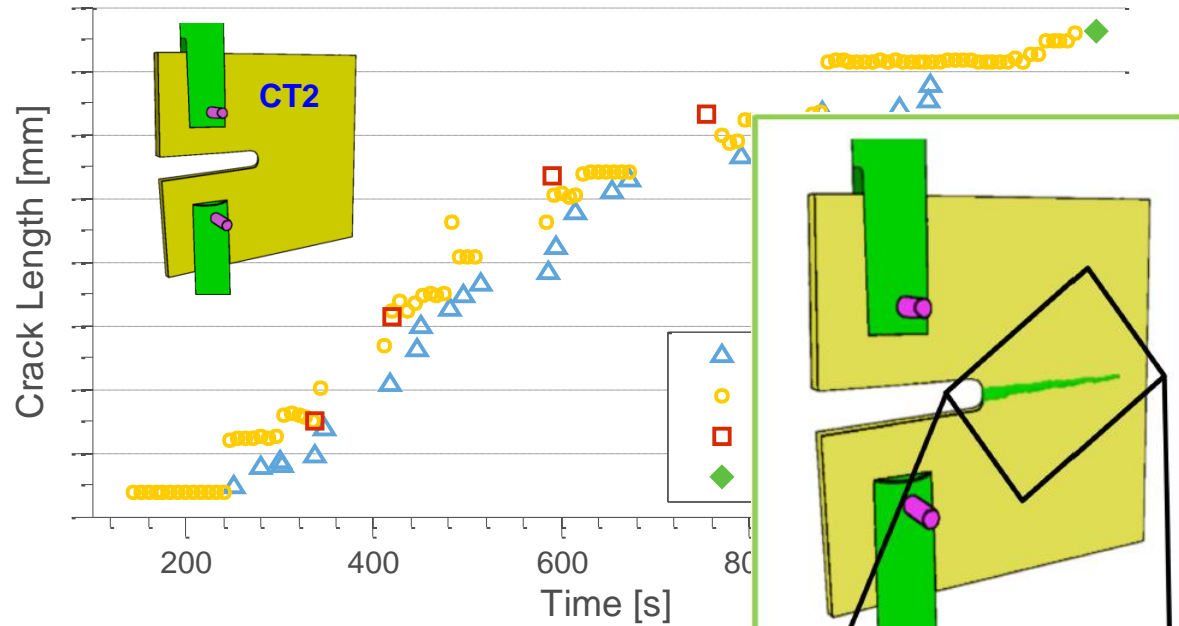
Crack propagation

Different measurement techniques

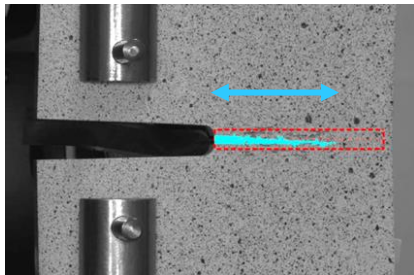
- Optical tracking (*grey level gradient*)
- DIC tracking (*discontinuity disp. field*)
- IR thermography (*heating crack*)
- X-Ray tomography (*ex and in-situ*)

Different measurement techniques

- Cross-check to \nearrow confidence
 - Complementary technique
- Surface, volume, ...*

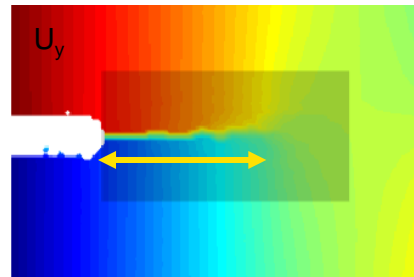


Optical tracking



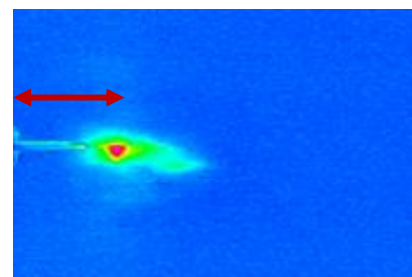
[Pack 17]
[Panin 17]

DIC tracking

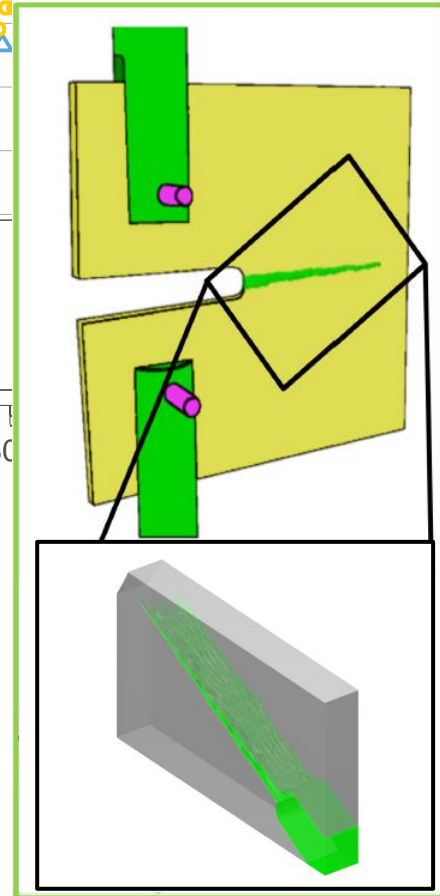


[Lopez-Crespo 08]
[Vanlanduit 09]
[Catalanotti 10]

IR Thermography



[Muller 16]
[Archer 17]



X-Ray tomography by
Safran Aircraft Engines

Crack propagation

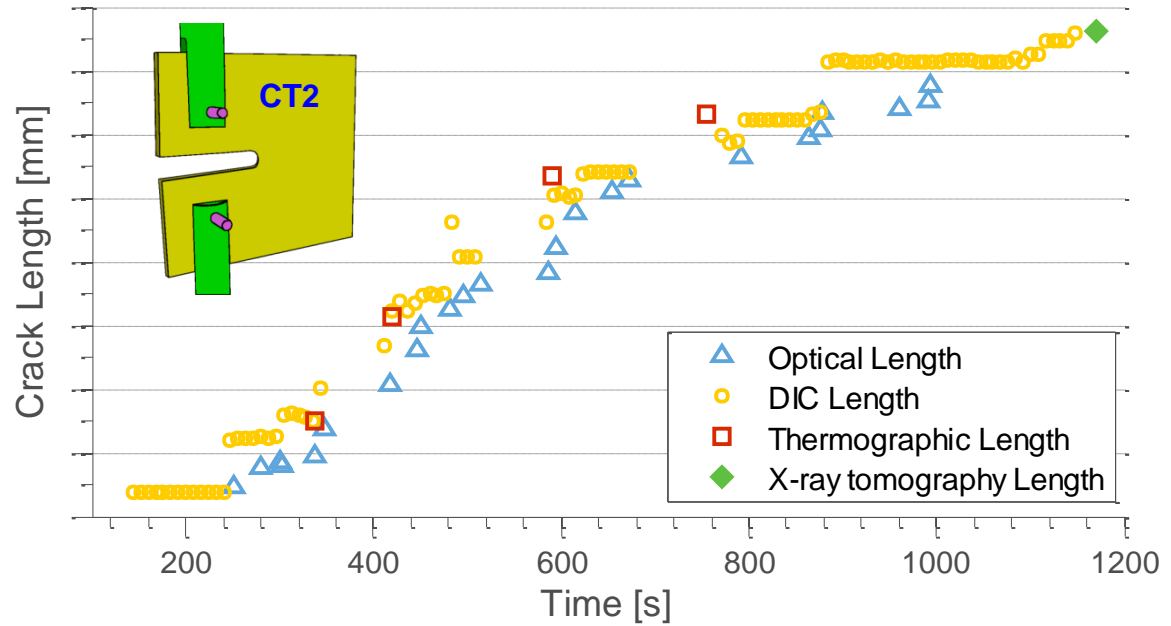
Different measurement techniques

- Optical tracking (*grey level gradient*)
- DIC tracking (*discontinuity disp. field*)
- IR thermography (*heating crack*)
- X-Ray tomography (*ex and in-situ*)

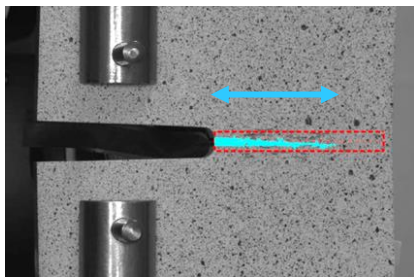
Different measurement techniques

- Cross-check to \nearrow confidence
- Complementary technique

Surface, volume, ...

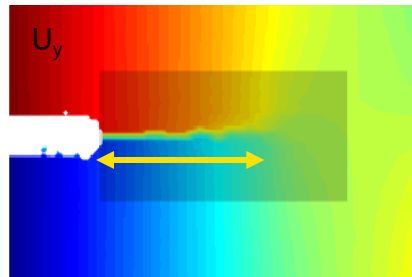


Optical tracking



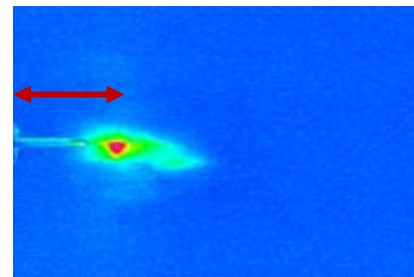
[Pack 17]
[Panin 17]

DIC tracking



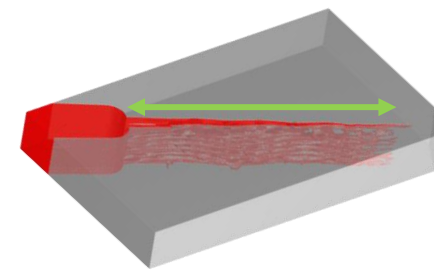
[Lopez-Crespo 08]
[Vanlanduit 09]
[Catalanotti 10]

IR Thermography



[Muller 16]
[Archer 17]

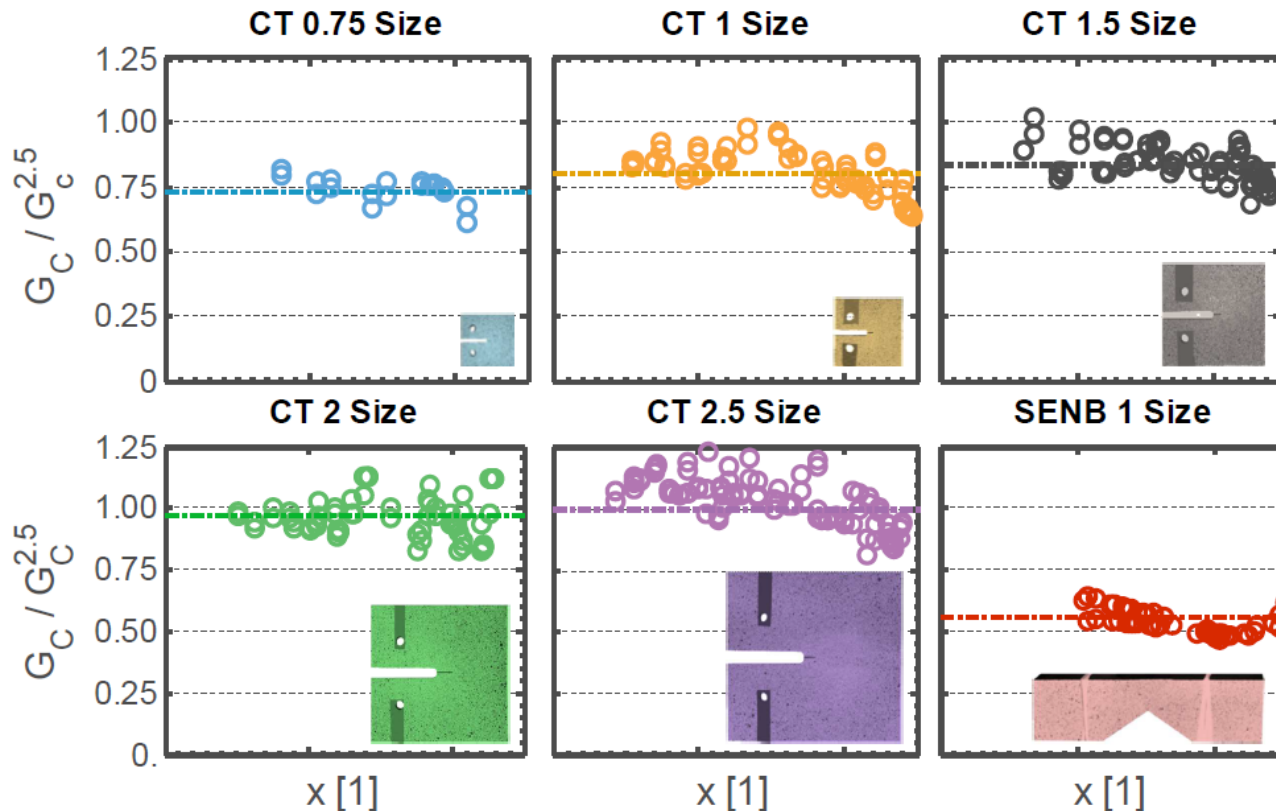
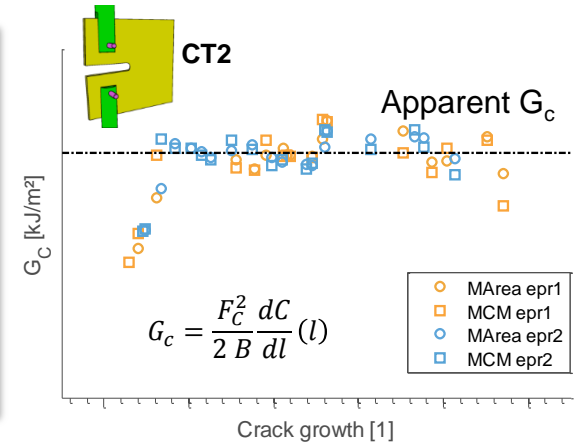
X-ray Tomography



X-Ray tomography by
Safran Aircraft Engines

Analysis of the available tests

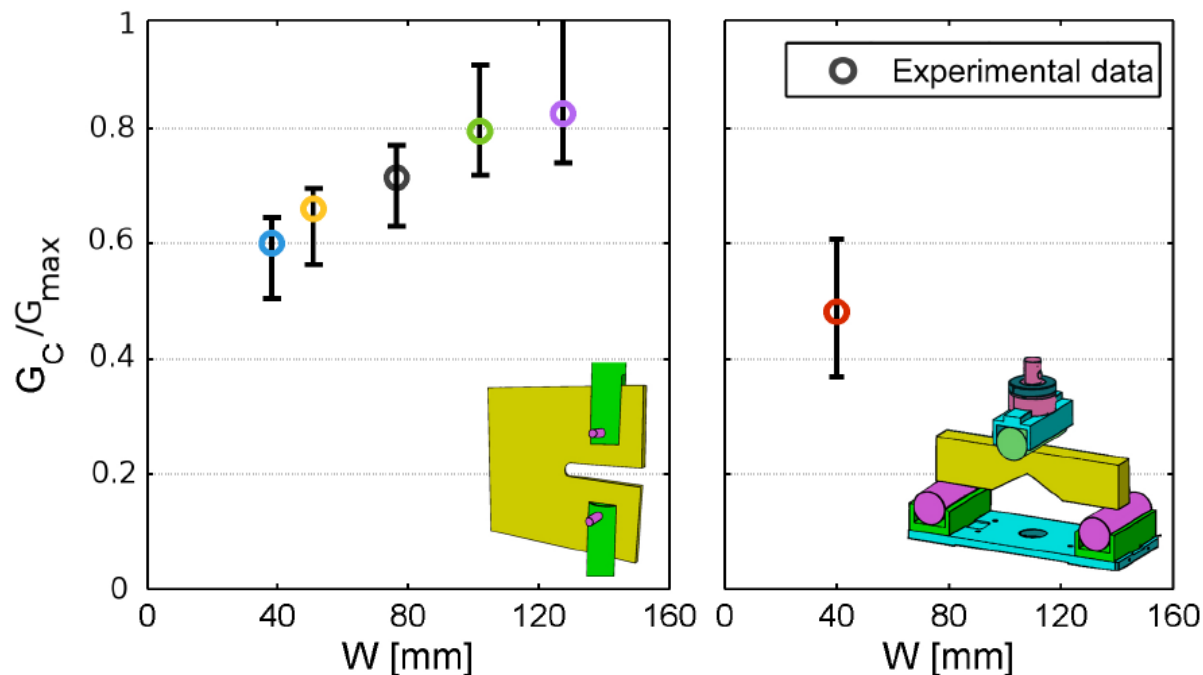
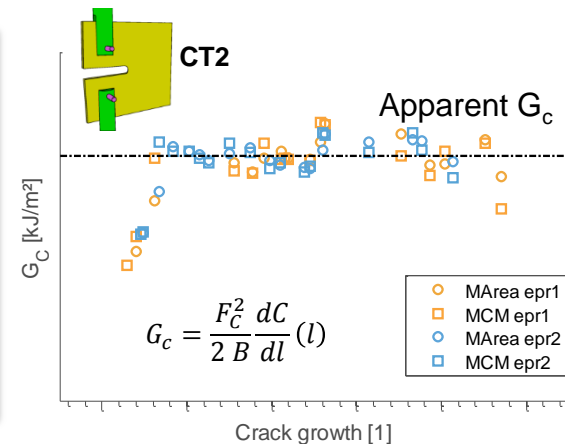
- G_c estimation for different sizes and types of specimens
 - Estimation with *Area Method* and the *Modified Compliance Method*
 - Evolution of apparent G_c as a function of the size of CT specimen
 - Different G_c for different types of specimens (CT and SENB)
- Use of LEFM is not relevant for 3D woven composites



[Medeau 17]

Analysis of the available tests

- G_c estimation for different sizes and types of specimens**
 - Estimation with *Area Method* and the *Modified Compliance Method*
 - Evolution of apparent G_c as a function of the size of CT specimen
 - Different G_c for different types of specimens (CT and SENB)
- Use of LEFM is not relevant for 3D woven composites**



[Medeau 17]

Scaling laws

Scaling laws (different sizes W) for materials without internal lengths [Bazant 93]

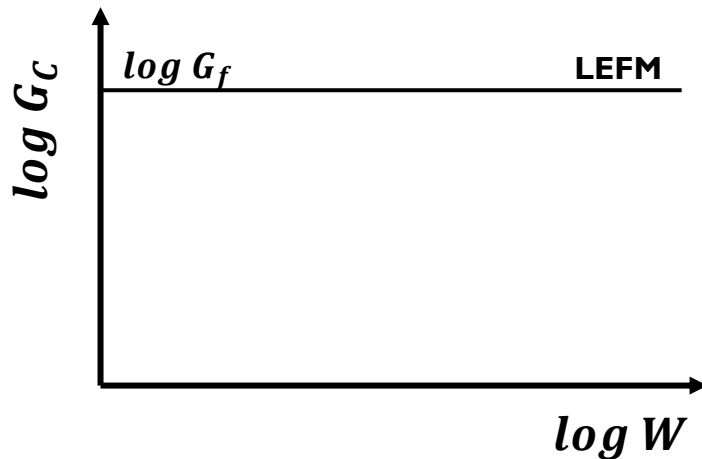
- With linear fracture mechanism: $\sigma_C \propto 1/\sqrt{W}$, $G_C \propto 1$ and $F_R \propto \sqrt{W}$
- With stress based model: $\sigma_C \propto 1$, $G_C \propto W$ and $F_R \propto W$

Scaling laws for materials with internal lengths

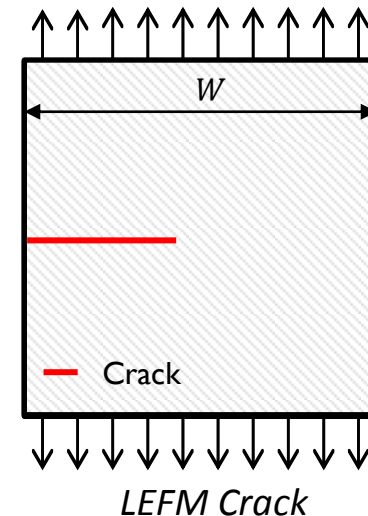
- Already available for concrete and rock [Bazant 84, 93]
- Introduction of internal length c_f linked to microstructure:

- G_f : asymptotic energy release rate when $W \gg c_f$
- W_0 : transition length depends on c_f and specimen geometry

$$G_c = \frac{G_f}{1 + \frac{W_0(c_f)}{W}}$$



Transition between LFEM/ stress model



Scaling laws

Scaling laws (different sizes W) for materials without internal lengths [Bazant 93]

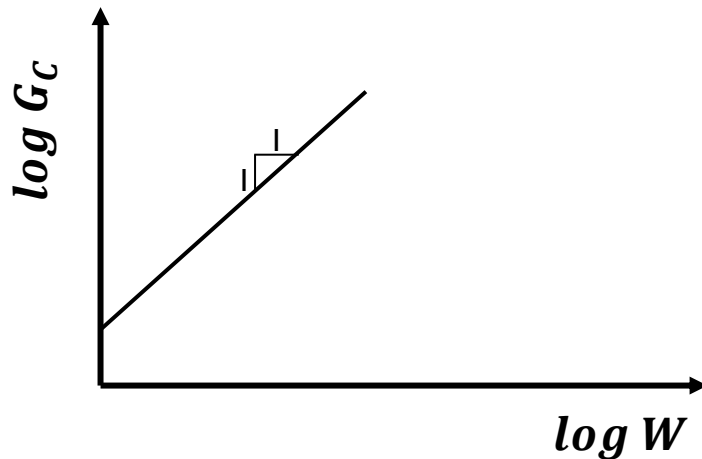
- With linear fracture mechanism: $\sigma_C \propto 1/\sqrt{W}$, $G_C \propto 1$ and $F_R \propto \sqrt{W}$
- With stress based model: $\sigma_C \propto 1$, $G_C \propto W$ and $F_R \propto W$

Scaling laws for materials with internal lengths

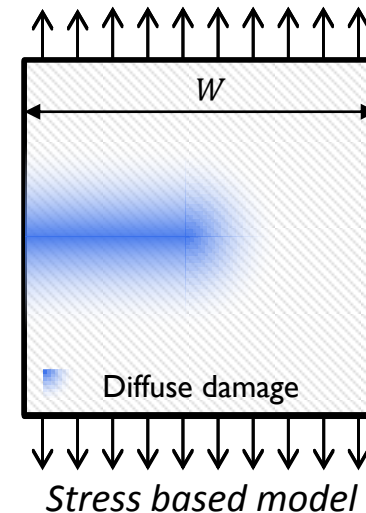
- Already available for concrete and rock [Bazant 84, 93]
- Introduction of internal length c_f linked to microstructure:

- G_f : asymptotic energy release rate when $W \gg c_f$
- W_0 : transition length depends on c_f and specimen geometry

$$G_c = \frac{G_f}{1 + \frac{W_0(c_f)}{W}}$$



Transition between LFEM/ stress model



Stress based model

Scaling laws

Scaling laws (different sizes W) for materials without internal lengths [Bazant 93]

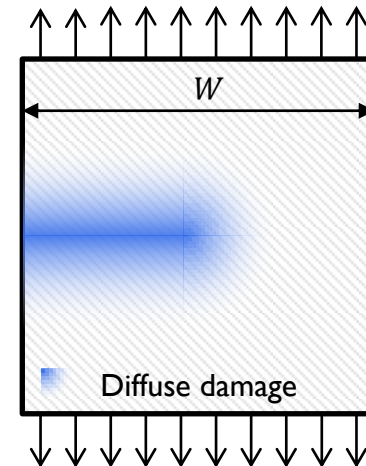
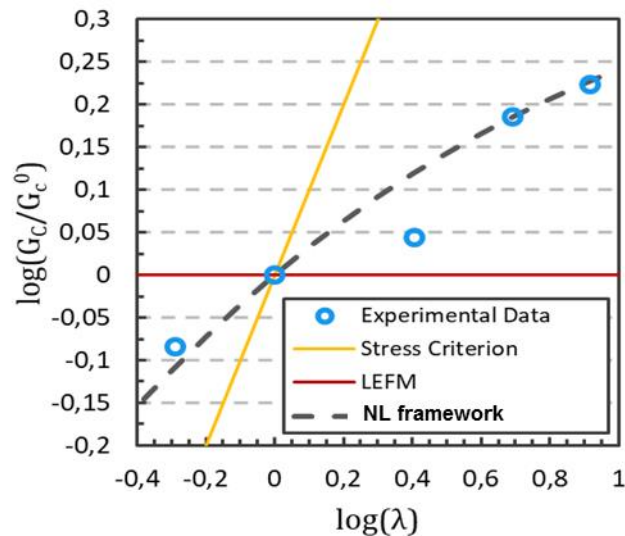
- With linear fracture mechanism: $\sigma_C \propto 1/\sqrt{W}$, $G_C \propto 1$ and $F_R \propto \sqrt{W}$
- With stress based model: $\sigma_C \propto 1$, $G_C \propto W$ and $F_R \propto W$

Scaling laws for materials with internal lengths

- Already available for concrete and rock [Bazant 84, 93]
- Introduction of internal length c_f linked to microstructure:

- G_f : asymptotic energy release rate when $W \gg c_f$
- W_0 : transition length depends on c_f and specimen geometry

$$G_C = \frac{G_f}{1 + \frac{W_0(c_f)}{W}}$$



Scaling laws

Scaling laws (different sizes W) for materials without internal lengths [Bazant 93]

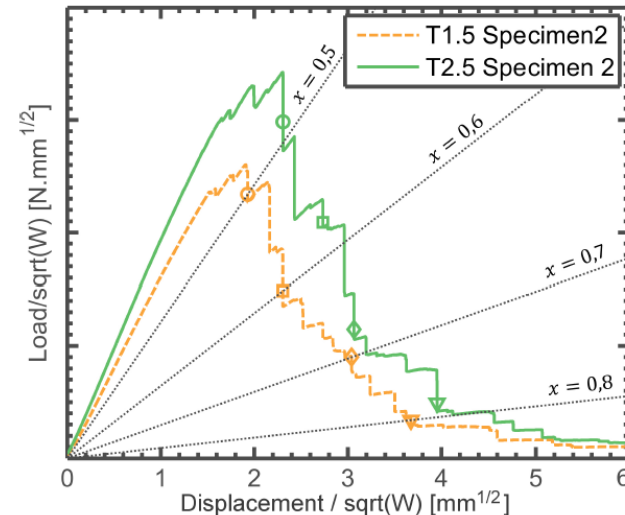
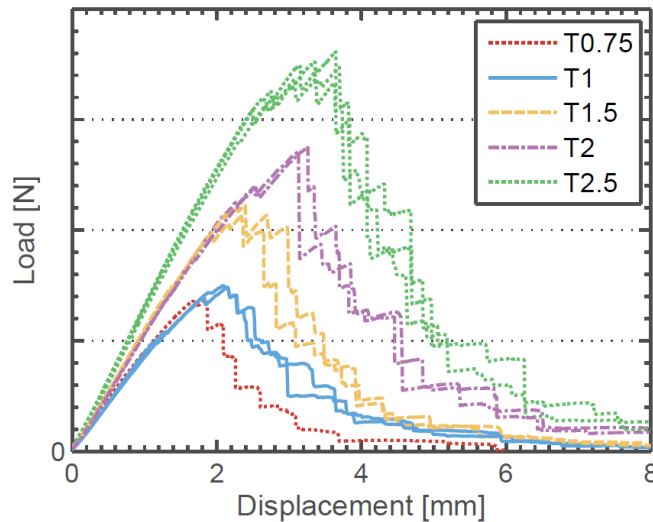
- With linear fracture mechanism: $\sigma_c \propto 1/\sqrt{W}$, $G_c \propto 1$ and $F_R \propto \sqrt{W}$
- With stress based model: $\sigma_c \propto 1$, $G_c \propto W$ and $F_R \propto W$

Scaling laws for materials with internal lengths

- Already available for concrete and rock [Bazant 84, 93]
- Introduction of internal length c_f linked to microstructure:

$$G_c = \frac{G_f}{1 + \frac{W_0(c_f)}{W}}$$

- G_f : asymptotic energy release rate when $W \gg c_f$
- W_0 : transition length depends on c_f and specimen geometry



Scaling laws

Scaling laws (different sizes W) for materials without internal lengths [Bazant 93]

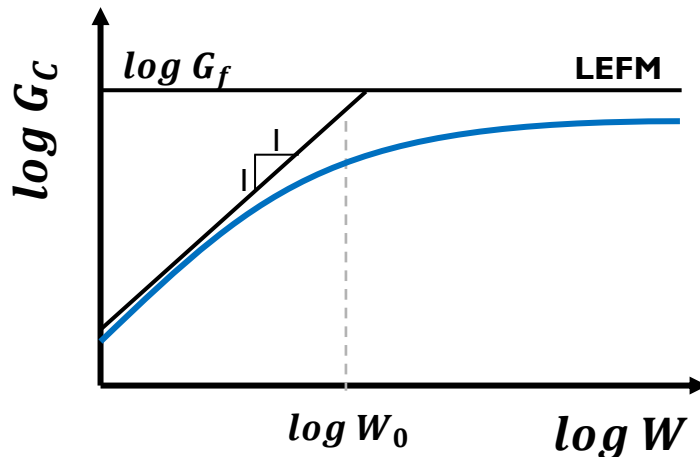
- With linear fracture mechanism: $\sigma_C \propto 1/\sqrt{W}$, $G_C \propto 1$ and $F_R \propto \sqrt{W}$
- With stress based model: $\sigma_C \propto 1$, $G_C \propto W$ and $F_R \propto W$

Scaling laws for materials with internal lengths

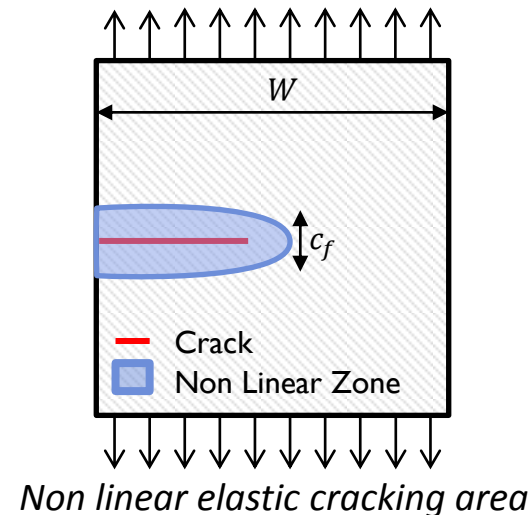
- Already available for concrete and rock [Bazant 84, 93]
- Introduction of internal length c_f linked to microstructure:

$$G_c = \frac{G_f}{1 + \frac{W_0(c_f)}{W}}$$

- G_f : asymptotic energy release rate when $W \gg c_f$
- W_0 : transition length depends on c_f and specimen geometry

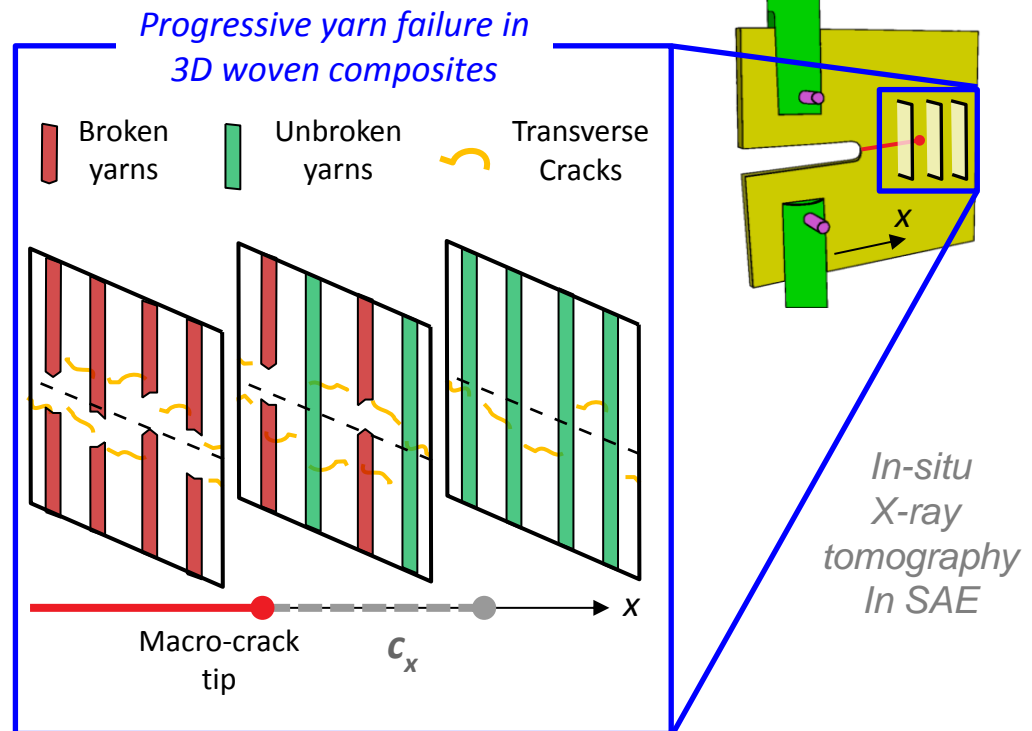
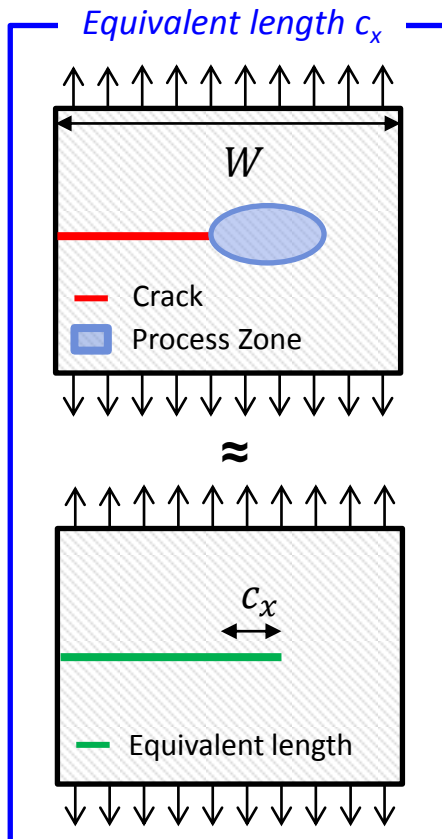


Apparent G_c evolution with NLFM



Internal lengths in 3D woven composites (1/2)

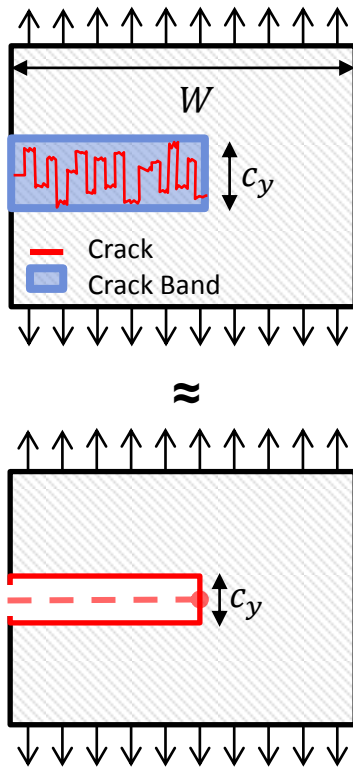
- Internal length along the crack path c_x
 - Progressive yarn cracking along the crack path highlighted using in-situ μ -tomography
 - Phenomenon guided by the architecture: linked to the inter-yarn length



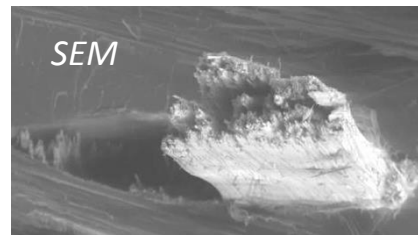
Internal lengths in 3D woven composites (2/2)

- Internal length along the crack path c_y
 - SEM and macro-pictures of the fracture profile exhibit a distribution of the yarn cracking length, associated with pull-out.
 - Measured on CT with different sizes: no variation with the specimen size

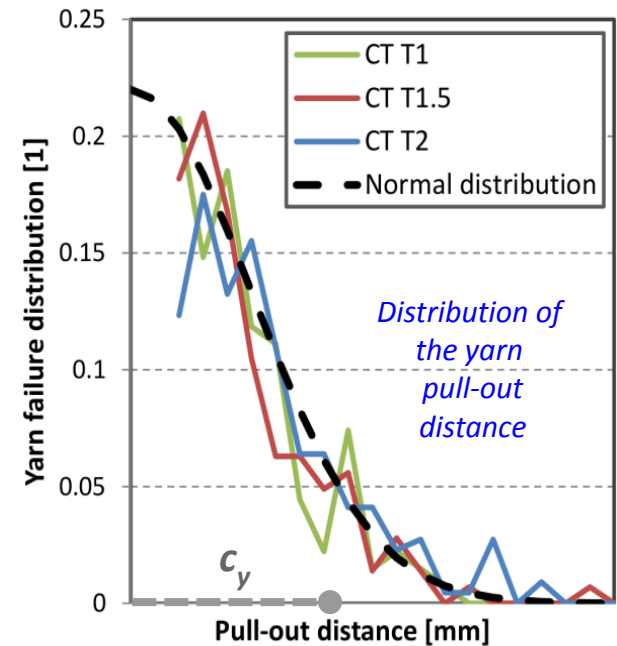
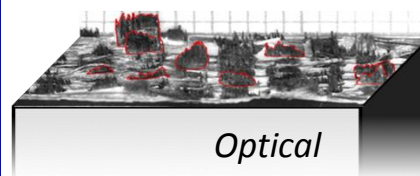
Equivalent length c_y

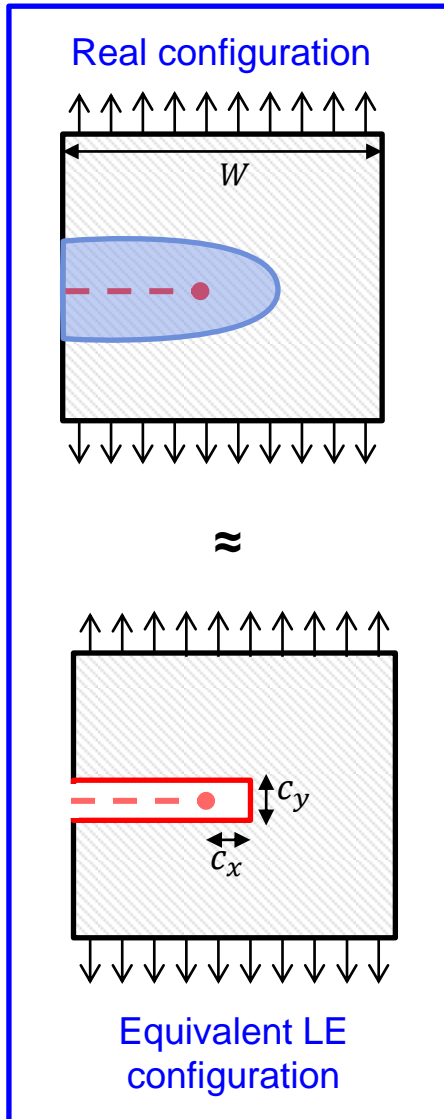


Experimental study on yarn pull-out



Yarn pull-out

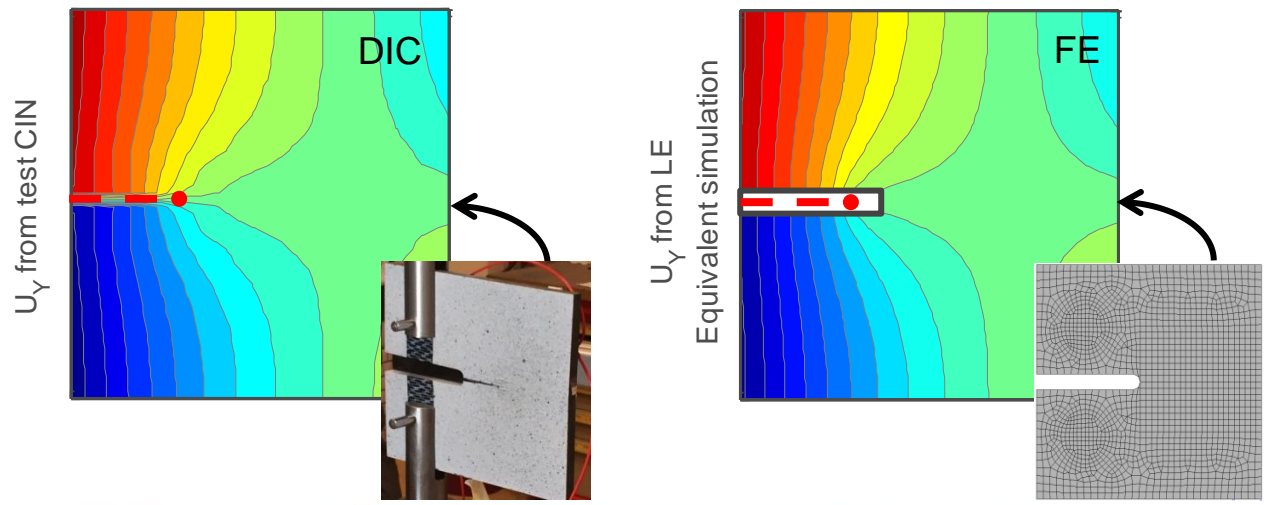




Non-linear framework

- LE equivalent configuration: Far field approximation
 - Determination of an equivalent configuration (c_x, c_y) providing the same effects away from the crack
- Determination of the critical energy release rate

$$G_c = \frac{F_C^2}{W} g\left(\frac{a}{W} + \frac{c_x}{W}, \frac{c_y}{W}\right) \cong \frac{G_f}{1 + \frac{\partial_x g(x) c_x}{g(x) W} + \frac{\partial_y g(x) c_y}{g(x) W}} \leftrightarrow \frac{G_f}{1 + \frac{W_0}{W}}$$
 - 3 material parameters to be identified (G_f, c_x, c_y)
 - A priori known parameters $(W, g(x), \partial_x g(x), \partial_y g(x))$
 $g(x)$ can be determined using linear elastic FE simulations



Validation of the proposed approach



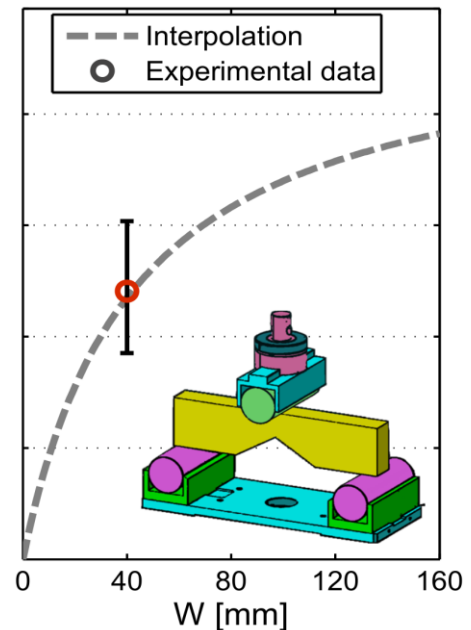
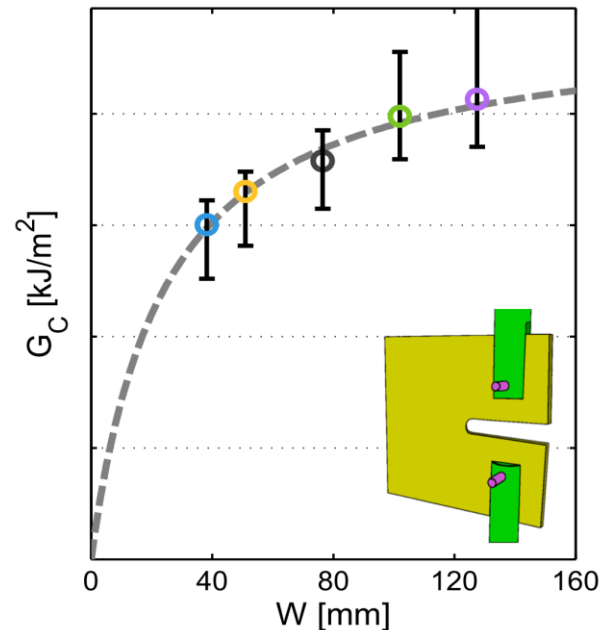
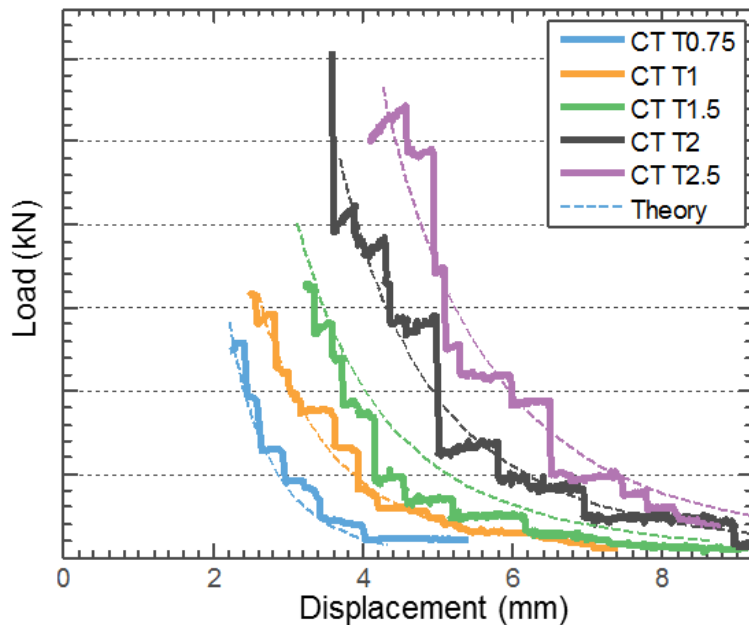
Identification protocol

- Determination through apparent G_C analysis of different tests (CT and SENB) of asymptotic critical energy release rate G_f and (c_x, c_y) strongly linked to the microstructure

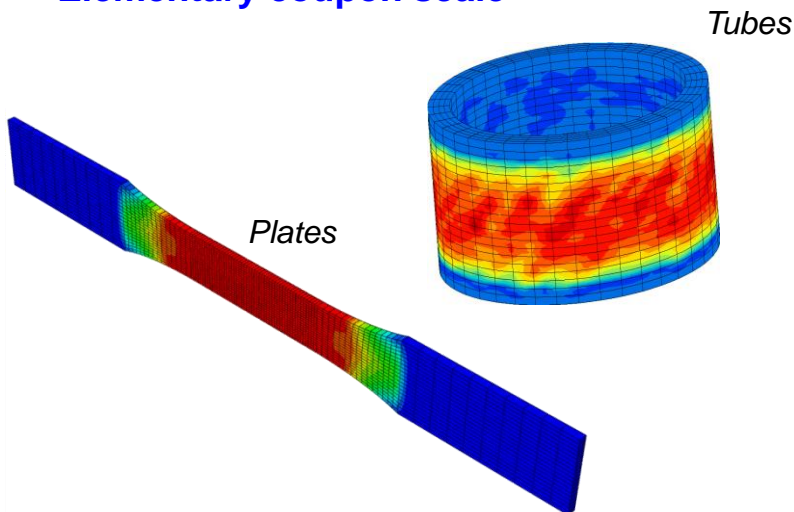


Validation of the proposed non-linear framework

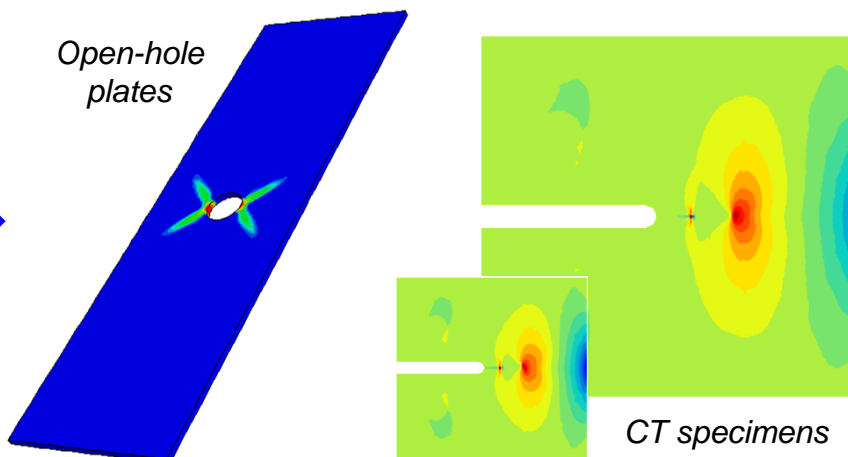
- Consistent evolution of the apparent G_C for different CT sizes
- Consistent prediction of the apparent G_C for different types of tests
- Good prediction of the load/displacement curves



Elementary coupon scale



Composite structure scale



Implementation in FE codes

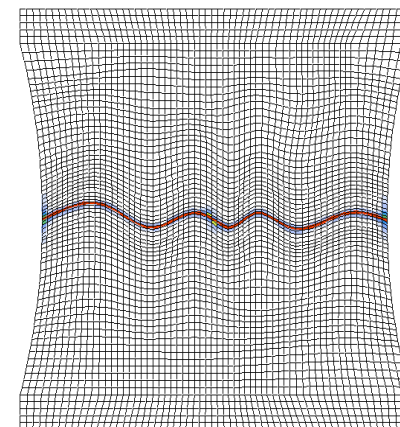
Robust implementation in finite element codes

- Implementation in a FE code with an implicit solver
- Softening behaviour after fibre yarn failure
- Avoid mesh dependence problem (size and orientation of elements)



Physically based regularization techniques

- Regularisation methods to avoid localisation problem
- Methods used in physical key quantities



Mesh dependency problem

Models considered in the numerical test campaign

Regularisation methods

- Simulations performed with  code in quasi-static
 - Delay effect methods  [Needleman 88], [Allix 97], [Suffis 03], [Berro 06]
 - Non local approach  [Pijaudier-Cabot 87], [Peerlings 96], [Lorentz 05]
 - Phase-field method  [Francfort Marigo 98], [Bourdin 00], [Miehe 10]

Analysis of key quantities

- Avoid localization problem/mesh dependence
- Predictive scale effect on load/displacement curves and apparent G_c

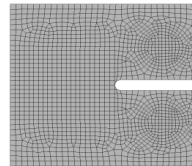
Geometry and mesh

Considered geometry

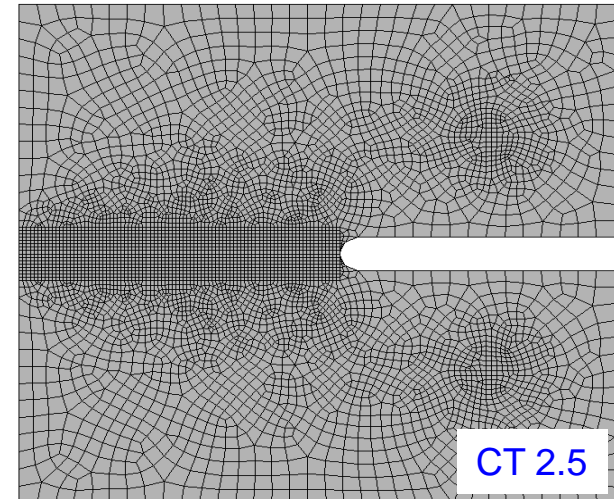
- Simulations performed on CT specimens with different sizes from 0.5 to 2.5

Considered meshes

- Fixed element size along the crack path whatever the specimen size



CT 0.5



CT 2.5

Delay effect methods

Principle of delay effect method

[Needleman 88], [Allix 97], [Suffis 03], [Allix 13] initially developed for *dynamic problems*

[Berro 06], [Marcin 10], [Hurmane 16] but also applied to quasi-static problems by other authors

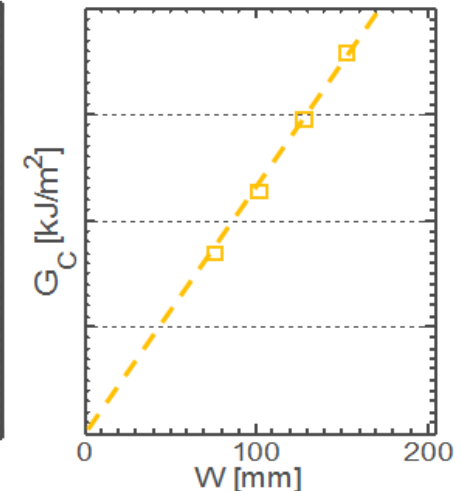
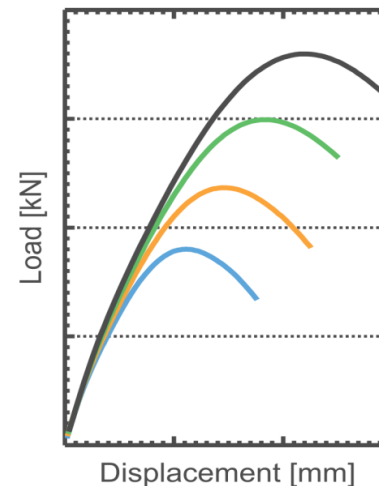
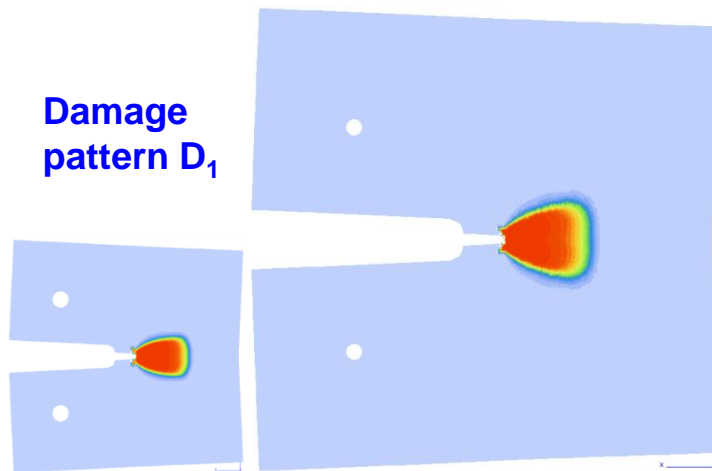
- Introduction of a delay effect τ on damage
- Avoid mesh dependence, easy to implement in FE code

$$\dot{D} = \frac{1}{\tau} (F(y) - D)$$

Scale effect predictions

- Evolution of failure load F_R as a function of W
- Linear evolution of the apparent G_c
- No internal length and energy control

→ **Delay effect provides inaccurate scale effect for 3D woven composites**



Delay effect methods

Principle of delay effect method

[Needleman 88], [Allix 97], [Suffis 03], [Allix 13] initially developed for *dynamic problems*

[Berro 06], [Marcin 10], [Hurmane 16] but also applied to quasi-static problems by other authors

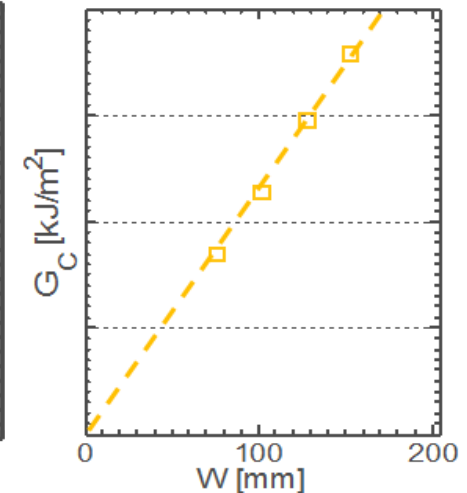
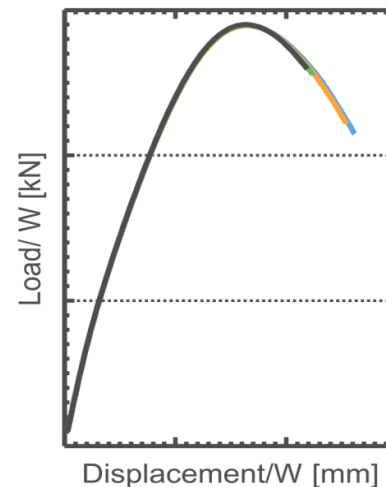
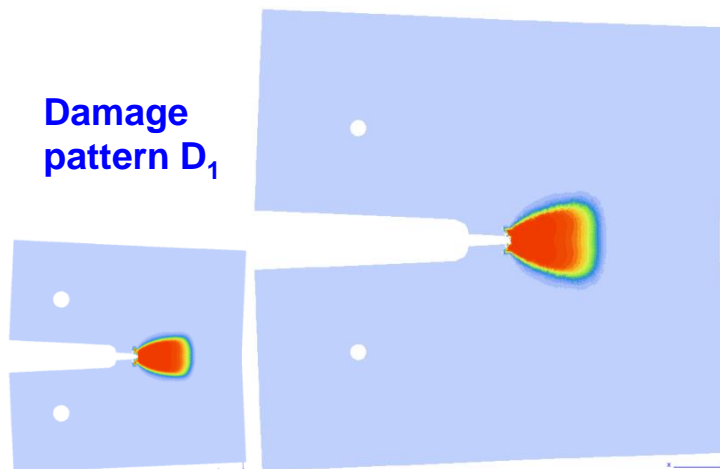
- Introduction of a delay effect τ on damage
- Avoid mesh dependence, easy to implement in FE code

$$\dot{D} = \frac{1}{\tau} (F(y) - D)$$

Scale effect predictions

- Evolution of failure load F_R as a function of W
- Linear evolution of the apparent G_c
- No internal length and energy control

→ **Delay effect provides inaccurate scale effect for 3D woven composites**



Non-local approach

Principle of non-local framework

[Pijaudier-Cabot 87], [Peerlings 96], [Lorentz 05], [Germain 06]

- Diffused damage in a volume defined by an internal length l
- Avoid mesh dependence, but **intrusive to FE code**

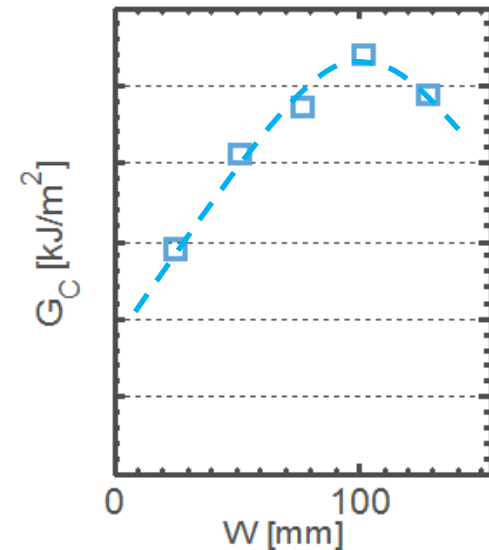
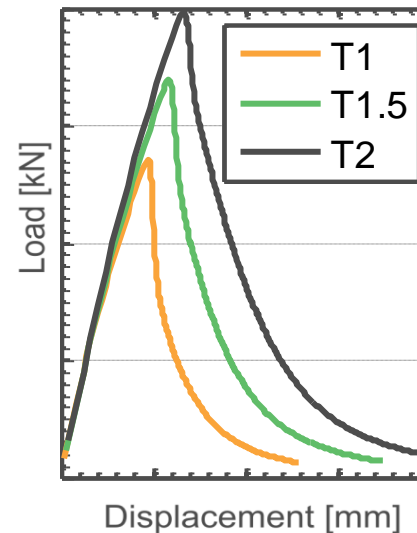
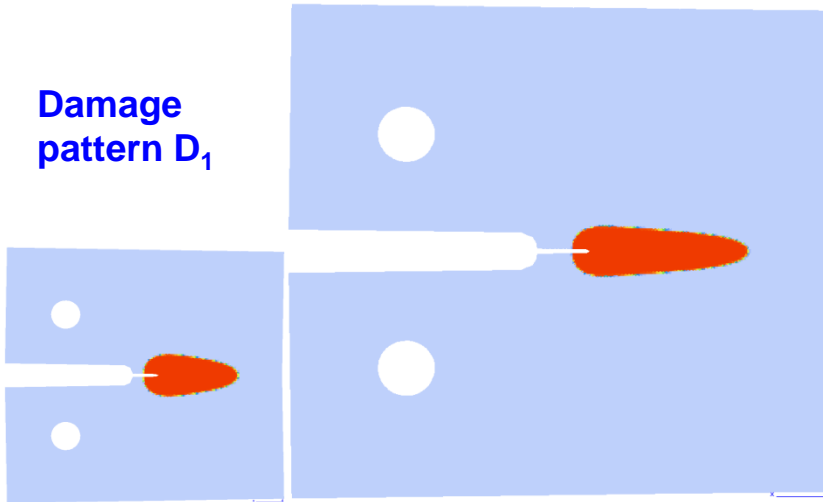
$$\bar{Y} - l^2 \nabla^2 \bar{Y} = Y(\varepsilon)$$

Scale effect predictions

- Complex evolution of failure load F_R and apparent G_C
- Internal length considered but no energy control
- No control of the crack failure pattern

→ **Non local qualitatively exhibits a relevant but complex scaling law**

Damage pattern D_1



Phase-field method

Principle of phase-field method

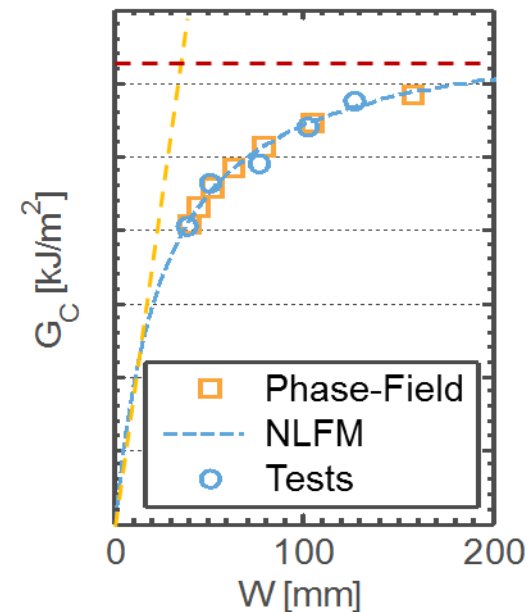
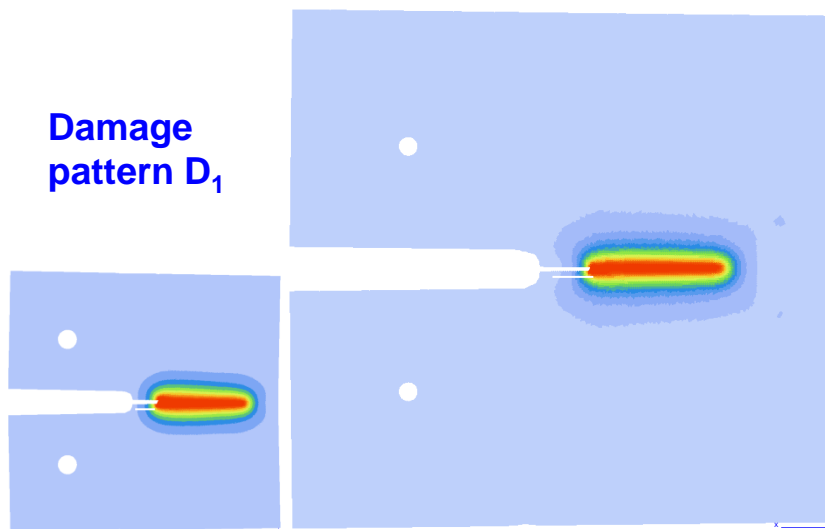
[Francfort Marigo 98], [Bourdin 00], [Miehe 10]

- Diffused damage D with the introduction of (G_c, l)
- Intrusive to FE code but **numerical difficulties**

$$D - l^2 \nabla^2 D = \frac{2l}{G_c} (1 - D) E_0 \varepsilon^2$$

Scale effect predictions

- Accurate evolution of failure load F_R and apparent G_c → **Phase-field exhibits the accurate scaling law for 3D woven composites**
- Internal lengths l and energy control G_c
- Control of the crack failure pattern



Phase-field method

Principle of phase-field method

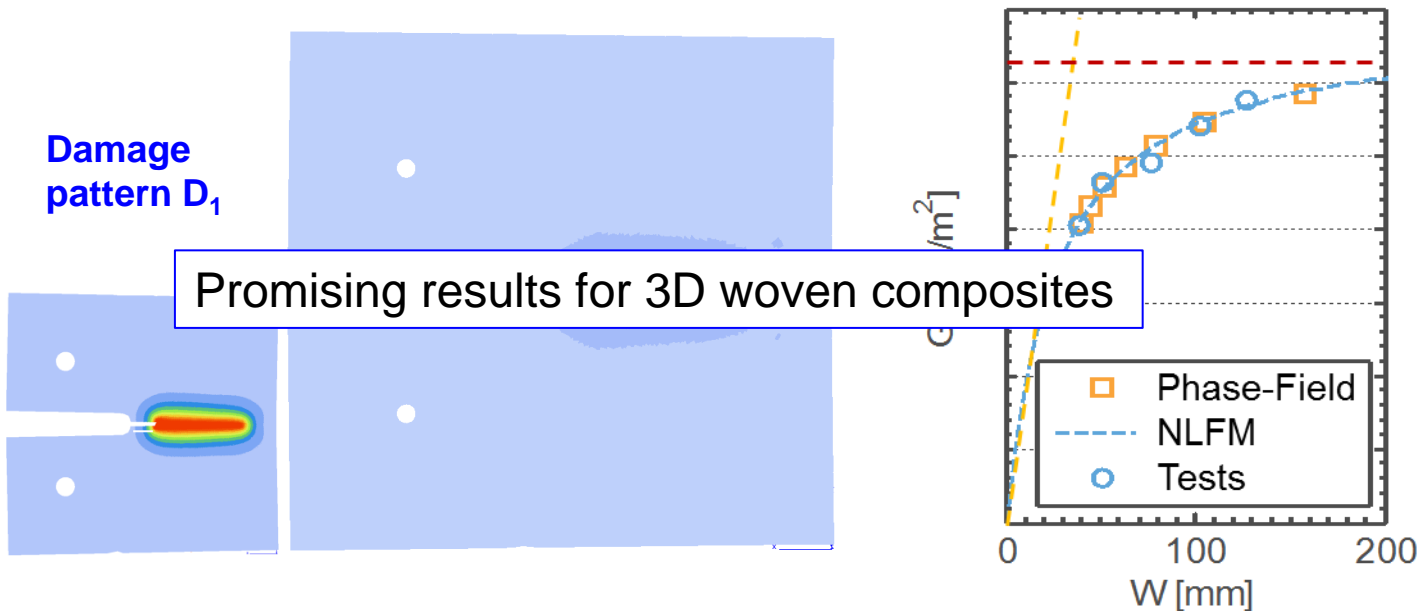
[Francfort Marigo 98], [Bourdin 00], [Miehe 10]

- Diffused damage D with the introduction of (G_c, l)
- Intrusive to FE code but **numerical difficulties**

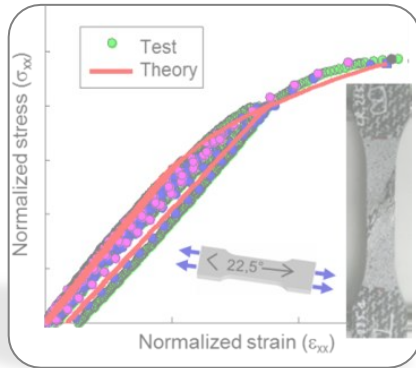
$$D - l^2 \nabla^2 D = \frac{2l}{G_c} (1 - D) E_0 \varepsilon^2$$

Scale effect predictions

- Accurate evolution of failure load F_R and apparent G_c → **Phase-field exhibits the accurate scaling law for 3D woven composites**
- Internal lengths l and energy control G_c
- Control of the crack failure pattern

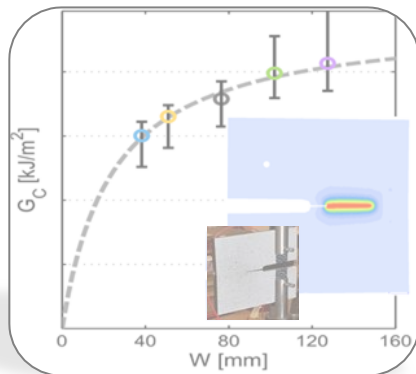


Promising results for 3D woven composites



Damage and failure model of elementary coupons

- Comprehension of the damage and failure mechanisms
- Proposition of a macroscopic damage and failure model
- Validation through comparisons with tests



Strength of composite structures with singularities

- Experimental study of progressive yarn failures
- Modelling of fibre yarn failure – physical key quantities
- Implementation of a softening behaviour in a FE code

**Conclusions
Perspectives**

Advantages and limitations of failure approach
Identification protocol – Validation tests

Conclusions

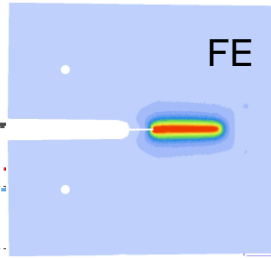
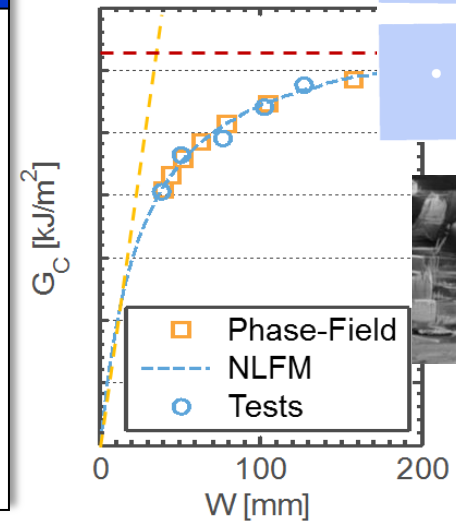
Damage mechanisms

- Diffuse damage oriented by microstructure in 3D woven composite
- Continuum damage model relevant for such a material
- Validation through comparisons with static/impact tests

Failure mechanisms

- Experimental study using CT and SENB tests
- Evolution of apparent G_c as a function of size and type of tests
- Non linear fracture framework relevant (energy + lengths)
- Phase-Field method promising for such a material

Fibre yarn failure



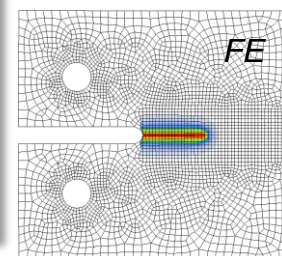
Perspectives

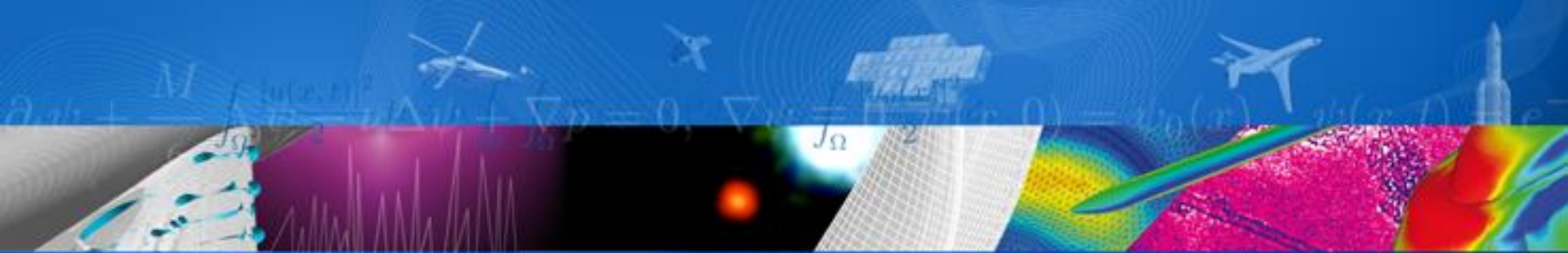
Experimental part

- Proposition of new configurations of test for validation
- Analysis tests with complex crack path (as in warp direction)
- Develop experimental device for CT tests in most reinforced direction

Numerical part

- Improve robustness of Phase-Field method in Zset code
- Application to other structures with different geometrical singularities





ONERA

THE FRENCH AEROSPACE LAB

r e t u r n o n i n n o v a t i o n

www.onera.fr